Rev.Adv.Mater.Sci. 17(2008) 1-32

SUBSTRATES FOR EPITAXY OF GALLIUM NITRIDE: NEW MATERIALS AND TECHNIQUES

S. A. Kukushkin[1], A. V. Osipov[1], V. N. Bessolov[2], B. K. Medvedev[3], V. K. Nevolin[3] and K. A. Tcarik[3]

[1]Institute of Mechanical Engineering Problems, Russian Academy of Sciences, V.O., Bolshoj pr., 61, St. Petersburg, 199178, Russia
[2] Ioffe Physico-Technical Institute, Russian Academy of Sciences, 26 Polytekhnicheskaya, St. Petersburg 194021, Russia
[3]Moscow Institute of Electronic Technology, Pas. 4806, bld.5, Zelenograd, 124498, Moscow, Russia

Received: December 10, 2007

Abstract. Different techniques for epitaxial growth of gallium nitride and main properties of GaN layers as well as devices made on the base of GaN-structures are described in the review. A new approach to suppression of the dislocation formation process along with reduction of elastic deformation of GaN in the case with gas phase chloride epitaxy on a Si(111) substrate due to application of an additional thin SiC-layer separated from a porous Si-interlayer is discussed.

1. INTRODUCTION

A skyrocketing progress in development of instruments based on gallium nitride has challenged the conventional thinking in requirements to materials used in successful construction of devices for micro- and opto-electrics. Up to date, there were unknown events of commercialization of semiconductor films, where only heteroepitaxial materials are used in their production. It was believed that in industry low-defect films of defect density below 10^6 cm^{-2} ought to be solely required [1], therefore nothing but solid substrates were used. However, as it was found quite recently, light-emitting diodes based on gallium nitride (GaN) grown on sapphire demonstrate perfect luminescence capacity, in spite of the fact that concentration of defects in this case is of 10^{10} cm^{-2} [2]. Actually, in contrast to most of semiconductors, the presence of dislocations in GaN does not cause fast degradation of optical or electric properties. So, sapphire was and it remains valid as the basic substrate in gallium nitride electronics. However, there are three causes opposed to call sapphire as "an ideal material" for using it in construction of electronic instruments based on GaN. They are the following: 1) the thermal expansion coefficient of sapphire is far higher than that GaN, and this leads to cracking of thick films [3]; 2) a rather large misfit of the substrate lattices (~16%) resulted in high concentration of defects; 3) sapphire is a dielectric, therefore, sapphire is often to be etched, and this is an additional laborious engineering problem.

In cases where a high density of dislocations does not influence upon work function of weak-current diodes, it becomes rather significant in production of more complicated apparatus such as lasers, diode lasers, heavy-current diodes and transistors, devices of high working range, and so on. It follows that although sapphire is not a rather universal substrate for gallium nitride electronics, its characteristics determine a fairly low quality limit for GaN prepared. Thus, at present, remarkable intensive search for new materials, which would be in good agreement with GaN relative to their lattices, thermal and electric properties for GaN epitaxy are carried out.

Physical properties of gallium nitride are promising in production of this material as a semicon-

Corresponding author: S.A. Kukushkin, e-mail:ksa@phase.ipme.ru

© 2008 Advanced Study Center Co. Ltd.

Table 1. Physical properties of GaN.

Property	Value for hexagonal structure	Value for cubic structure
Forbidden band width at 300K ,eV	3.44	3.4
Electron mobility maximum, cm^2/V s		
300K	1350	
77K	19200	
Hole mobility maximum at 300K, cm^2/V s	13	
Range of semiconductor doping, cm^{-3}		
electronic	from 10^{16} to $4 \cdot 10^{20}$	
hole	from 10^{16} to $6 \cdot 10^{18}$	
Melting point, K	2773	2770
Lattice constants at 300K		
a, nm	0.318843	0.452
c, nm	0.518524	
Change in lattice constants when heating at 300 up to 1400K	$\Delta a/a_0$ 0.5749, $\Delta c/c_0$ 0.5032	
Specific thermal conductivity at 300K, Wt/cmK	2.1	1.3
Thermal capacity at 300K, J/moleK	35.3	34.1
Modulus of elasticity, GPa	210 ± 20	204 ± 25
Hardness(nanoindentation) at 300K, GPa	15.5 ± 0.9	
Microhardness at 300K, GPa	10.8	
Young's modulus at 1000K, MPa	100	80

ductor in many electronic and optoelectronic instruments [4,5]. Its wide and direct band gap is an ideal one for short-wave emitters (light-emitting diodes and diode lasers) and detectors. Due to a wide band gap and high thermal stability of GaN, the material is indispensible for production of high-temperature and high-power units. Gallium nitride constitutes solid solutions both with aluminum nitride (AlN) and indium nitride (InN) providing a very wide range of energy band gap (1.9-6.2 eV). Such ability to build up solid solutions plays a key role in construction of short-wave emitters and heterostructures with high potential barrier. In addition, gallium nitride possesses a high piezoelectric effects; this property is determinative one in production of heterostructural transistors. Main physical characteristics of gallium nitride are enumerated, in Table 1.

Gallium nitride in its native state is of hexagonal wurtzite structure with $P6_3mc$ space group. The wurtzite structure consists of alternate biatomic close-packed layers Ga and N (0001) in ABABAB sequence [7]. Crystal structure of hexagonal GaN along [0001], [11-20], [10-10] axes is shown in Fig.1.

Cubic GaN-structure (F-43m space group) may be stabilized in epitaxial films. Close-packed (111) planes are following as ABCABC in the structure. Crystal structure of cubic GaN along [100], [110], [111] axes is shown in Fig.2.

Lattice constants GaN versus temperature dependences are given in Figure 3 according to data obtained from Ref. [8].

2. SUBSTRATES FOR EPITAXY OF GAN

2.1. Potential substrates and problems with heteroepitaxy

Since three-dimensional crystals of GaN are not produced on a commercial scale, most of investigators rely only on heteroepitaxy in preparation of devices based on GaN, it is necessary to choose the crystals with lattice parameters, chemical and

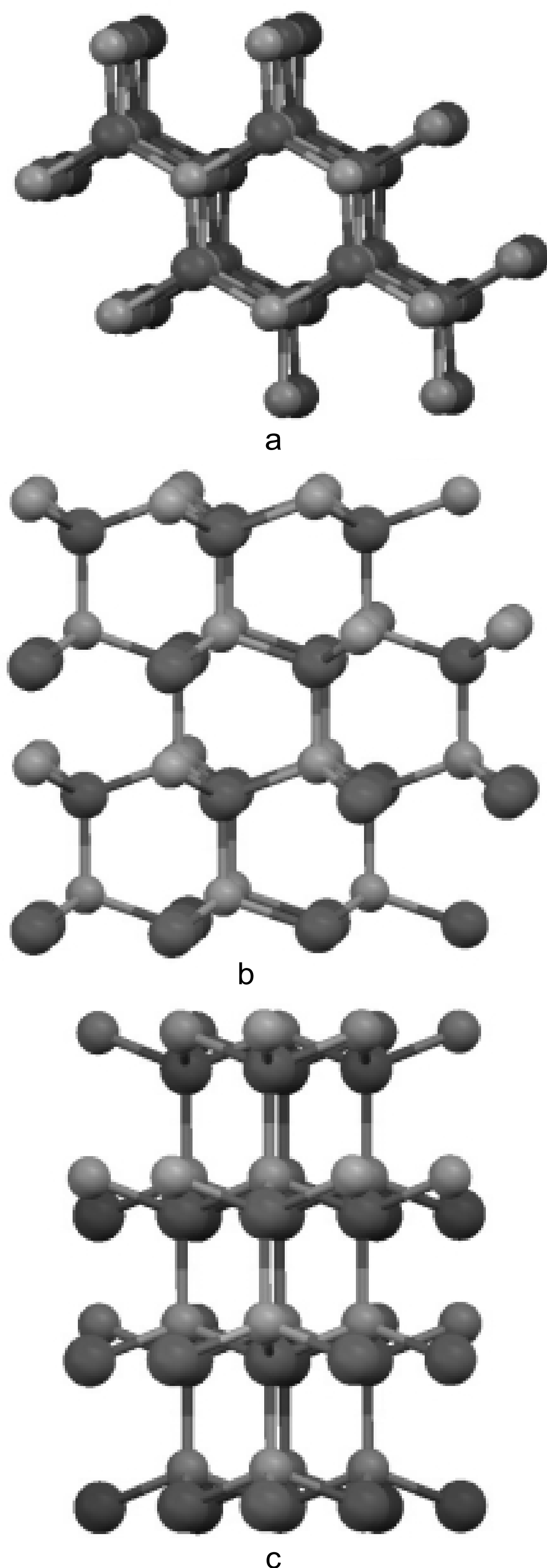

Fig 1. Crystal structure of hexagonal GaN along: (a) [0001]; (b) [11-20]; and (c) [10-10].

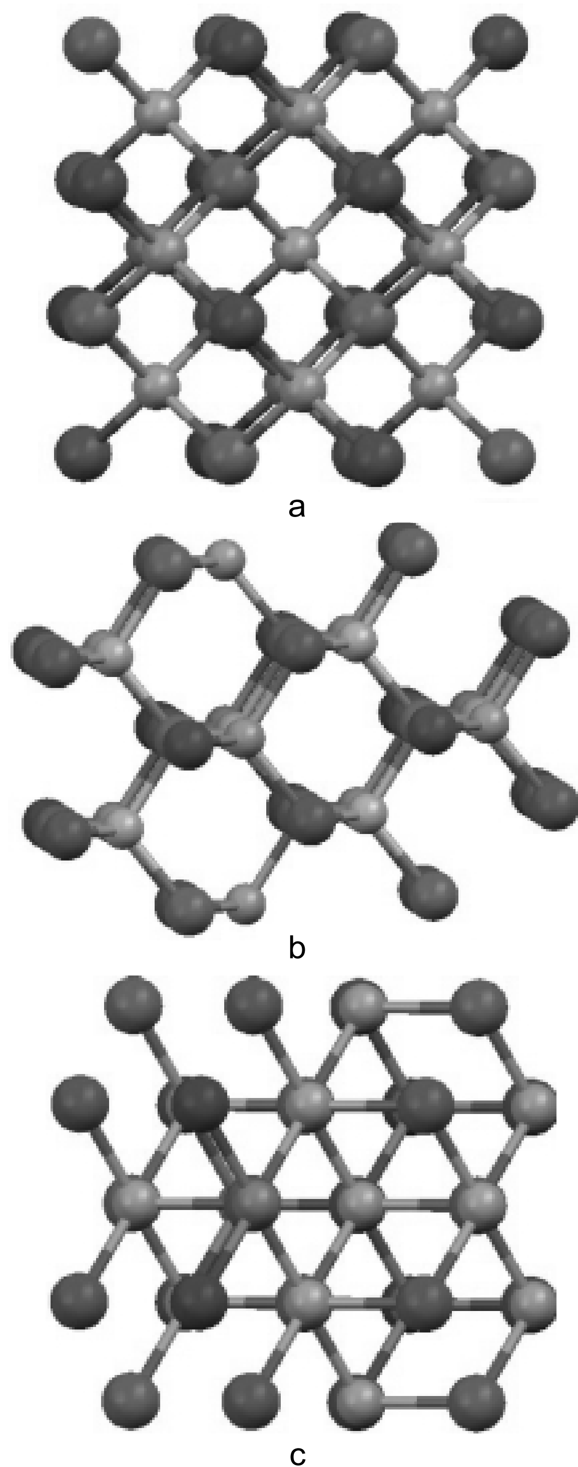

Fig 2. Crystal structure of cubic GaN along: (a) [100]; (b) [110]; and (c) [111] -directions.

physical characteristics correlated with development of in the cases of crystal film growth on foreign substrates. Most commonly, the mismatch parameter of substrates becomes a main criterion in selection of a substrate. In this connection, a

Table 2. Properties of some applicants to substrates for GaN.

Material	Structure	Space group	Lattice constans (nm)		
			a	*b*	*c*
Semiconductors					
w-GaN	Wurtzite	$P6_3mc$	0.31885		0.5185
zb-GaN	Zink-blende	$F\bar{4}3m$	0.4511		
r-GaN	Rock salt	$Fm\bar{3}m$	0.422		
w-AlN	Wurtzite	$P6_3mc$	0.31106		0.49795
zb-AlN	Zink-blende	$F\bar{4}3m$	0.438		
r-AlN	Rock salt	$Fm\bar{3}m$	0.404		
ZnO	Wurtzite	$P6_3mc$	0.32496		0.52065
β-SiC	3C (ZB)	$F\bar{4}3m$	0.43596		
SiC	4H (W)		0.3073		1.0053
SiC	6H (W)	$P6_3mc$	0.30806		1.51173
BP	Zink-blende	$F\bar{4}3m$	0.4538		
GaAs	Zink-blende	$F\bar{4}3m$	0.56533		
GaP	Zink-blende	$F\bar{4}3m$	0.54309		
Si	Of diamond	Fd3m	0.54310		
Silicon dioxides and sulfides					
Al_2O_3 (sapphire)	Rhombohedral	$R\bar{3}c$	0.4765		1.2982
$MgAl_2O_4$ (spinel)		$Fd\bar{3}m$	0.8083		
MgO	Rock salt	$Fm\bar{3}m$	0.421		
$LiGaO_2$	Prismatic	$Pna2_1$	0.5402	0.6372	0.5007
γ-$LiAlO_2$		$P4_12_12$	0.5169		0.6267
$NdGaO_3$	Prismatic	$Pna2_1$	0.5428	0.5498	0.771
$ScAlMgO_4$		$R\bar{3}m$	0.3236		2.515
$Ca_8La_2(PO_4)_6O_2$	apatite	R3mR	0.9446		0.6922
MoS_2		$P6_3mc$			
$LaAlO_3$	Rhombohedral	$R\bar{3}c$	0.5364		1.311
(Mn, Zn) Fe_2O_4	spinel	$Fd\bar{3}m$	0.85		
Metals and metal nitrides Hf	Hexagonal close packing HCP	$P6_3mc$	0.318		0.519
Zr	HCP	$P6_3mc$	0.318		0.519
ZrN	Rock salt	$Fm\bar{3}m$	0.45776		
Sc	HCP	$P6_3mc$	0.3309		0.54
ScN	Rock salt	$Fm\bar{3}m$	0.4502		
NbN	Rock salt	$Fm\bar{3}m$	0.4389		
TiN	Rock salt	$Fm\bar{3}m$	0.4241		

great number of material including metals, metal oxides, metal nitrides as well as semiconductors was investigated. Data on crystal structures and lattice constants for some applicants to substrates for GaN are collected in Table 2.

However, it turned out in practice, not only lattice constants are great significance, but also the structure of crystal material, treatment of a surface, composition, reactivity of the surface, as well as, chemical, thermodynamic and electric properties of the material used, have a great influence upon selection of materials for preparation of the substrates. It should be mentioned that the influence in most cases could be exhibited quite unexpectedly. Just a substrate determines crystal orientation, polarity, polytype, surface morphology, elastic

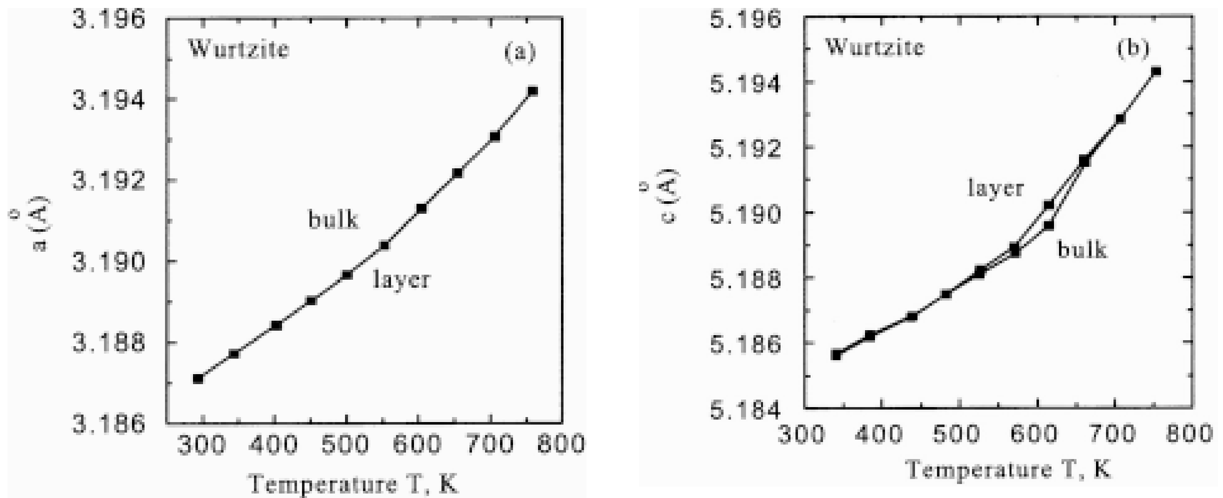

Fig 3. Temperature dependence of lattice constants of wurtzite GaN, see Ref. [8].

Table 3. Defects of film structures arising in the course of heteroepitaxy of compounds in the presence of great differences in crystallographic physical, chemical or mechanical properties of the compounds used as the base of devices produced.

Substrate property	Consequence for a substrate
Lateral mismatch of lattices	High-tension leakage currents of an unit due to high density of dislocations; short life times of minority charge carriers; decrease in specific thermal conductivity; accelerated diffusion of impurities
Vertical mismatch of lattices	Counter-phase interfaces; boundaries of inversion domains
Surface steps in non-isomorphous substrates	Mismatch boundaries of packing
Descrepancy between thermal conductivity coefficients	Strain thermally induced in a film
Low thermal conductivity coefficient	Weak dissipation of heat
Difference in chemical composition as compared to that of an epitaxial film	Contamination of film with substrate elements; boundary electronic stales made by broken bonds; poor wetting of a substrate with growing film
Nonpolar surface	Mixed polarities in an epitaxial film

strains, and concentration of gallium nitride defects. Thus, the substrate fully estimates, whether an instrument can acquire one or another quality.

Influence of a substrate on polarity and polarization of the third group nitrides grown epitaxially is enormous. In many cases, just the substrate controls polarity of a crystal as well as the sign and value of elastic strains of a growing epitaxial layer. Gallium nitride of [0001] orientation grows on most of the substrates. Nevertheless, an attention to crystals of some other orientation all the time increases just to weaken the role action of polarization effects. Note that piezo-effects can play a great part as well. Problems associated with heteroepitaxy are generalized in Table 3.

Regardless of substrate selection, there are many techniques to improve quality of growing crystal. They include treatment of crystal surface, for

Table 4. Main physico-mechanical properties of sapphire.

Property	Value	Range
Lattice constant (nm)	a=0.4765, c=1.2982	20 °C
Melting point (°C)	2030	
Density (g/cm^3)	3,98	20 °C
Thermal expansion coefficients (K^{-1})	6.66 10^{-6} || c-axis	20-50 °C
	9.03 10^{-6} || c-axis	20-1000 °C
	5.0 10^{-6} ⊥ c-axis	20-1000 °C
Percentages change in lattice constants	a/a_0 =0.83, c/c_0 =0.892	Heating from 293 to 1300K
Thermal conductivity (W/cm K)	0.23 ||c-axis	296K
	0.25 ||a-axis	299K
Heat capacity (J/K mol)	77,9	298K
Young's modulus (GPa)	452–460 in [0 0 0 1] direction 352-484 in the direction [1 1 -2 0]	
Tensile strength (MPa)	190	300K
Poisson's ratio	0.25–0.30	300K
Hardness Knoop Nanoindentation (GPa)	23.9 ±2.0	300K
Dielectric constants	8.6 ||c-axis	10^2 - 10^8 Hz
	10.55 ||a-axis	10^2 - 10^8 Hz
Refractive index	1.77 at λ = 577 nm	
Energy band gap (eV)	8.1–8.6	300K
Experimental value Resistivity (Ω cm)	> 10^{11}	300K

instance, by means of azotization, applying of a low temperature intermediate AlN-layer, using of multi-layer buffer system [9] and pendeo-epitaxy [10,11] as well as some other contrivances [12-14]. By means of all above-mentioned methods, the density of dislocations can be decreased from 10^{10} to 10^7 cm^{-2}. However, in industry even lower values of the dislocation density are needed for manufacture of complex apparatus operating under extreme conditions of temperature, voltage or electric current. So, in order to describe the whole of a gallium nitride potential, as a wide-band gap semiconductor, it is necessary to find, in principle, new substrate, which ought to guarantee the highest quality of epitaxial layers.

2.2. Sapphire

Sapphire, i.e. single crystal of (Al_2O_3), was used in pioneer technology of GaN epitaxy even in 1969, and up to date, sapphire remains the substrate for epitaxy of GaN, which is most commonly, used great mismatch (~16%) between lattices of sapphire (Al_2O_3) and GaN results in high concentration of dislocations of the mismatch namely, (10^{10} cm^{-2}). Such a great value leads to decrease in mobility of charge carriers and the lifetime of minority charge carriers, along with the above directions; this value gives rise to increase in thermal conductivity that, in its turn, causes progressive degradation of apparatus. The thermal expansion coefficient of sapphire is higher than that of GaN, and, in such a way, biaxial compressive strain arises in an epitaxial layer upon cooling. Temperature dependence of a mismatch parameter between (Al_2O_3) and GaN- lattices is given in Fig. 4 by Ref. [14].

As for thick films, this leads to cracking. Since the thermal conductivity coefficient of sapphire, ~ 0.25 Wt/cm K at 100 °C, this fact manifests in a rather poor dissipation of heat, as compared to

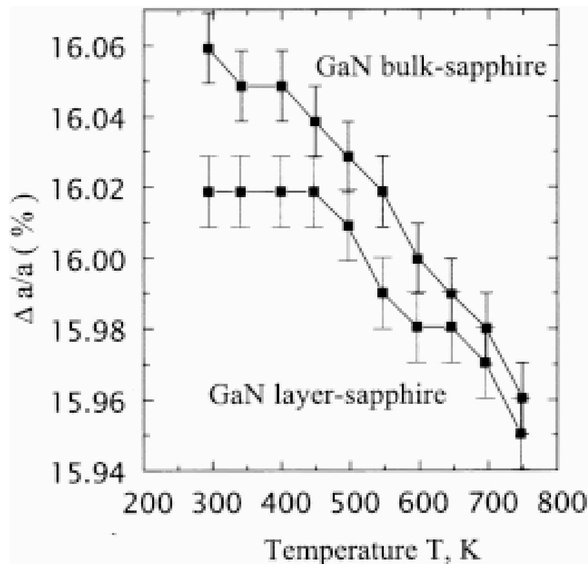

Fig 4. Temperature dependence of a mismatch parameter between Al_2O_3 - and GaN-lattices.

other substrates. Another limitation of sapphire lies in dielectric characteristics of sapphire. Therefore, the electric contact should be mounted on the front side of an instrument; in this case working area of the instrument is reduced and, in addition, the engineering procedure is, sharply, complicated. Along side with the above mentioned, there are data proving that oxygen of sapphire penetrates into gallium nitride, and this leads to decline in electron characteristics of the latter.

Sapphire has R-3c space group and it consists predominantly of ionic bonds. Sapphire can be described the both as rhombohedral and elementary hexagonal cell. In a rhombohedral cell of 84.929 Å^3 in volume there are 10 atoms, namely 4 ions of Al^{3+} and 6 ions of O^{2-}, whereas a hexagonal cell of 254.792 Å^3 in volume contains 30 atoms, namely, 12 ions of Al^{3+} and 18 ions of O^{2-}. Note that main surfaces where gallium nitride is growing are non-polar. Picture of hexagonal lattice of sapphire along [001], [1-100], [11-20] directions is represented in Fig.5.

Presently, solid single crystals of sapphire are growing by a few techniques, and nearly all of single crystals grown by such methods (apart from the most fast ones) are of high quality. Concentration of defects is of the order of 10^3 sm^{-2} in them. Up to date, on transition of the defects of sapphire into

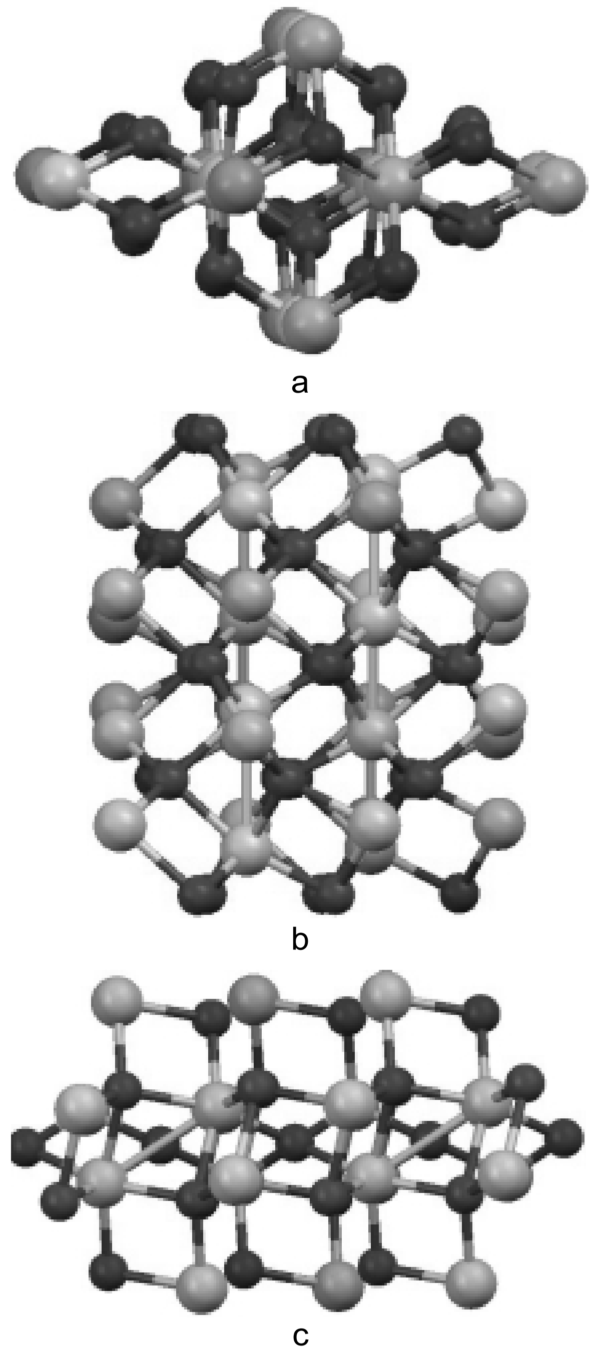

Fig. 5. Structure of hexagonal Al_2O_3 crystal along: (a) [0001]; (b) [1-100]; (c) [11-20].

GaN are absent in literature. Below data on sapphire properties are collected in [15] Table 4.

2.3. Silicon carbide

Silicone carbide SiC has a number of advantages over sapphire for GaN growing. First of all, the lat-

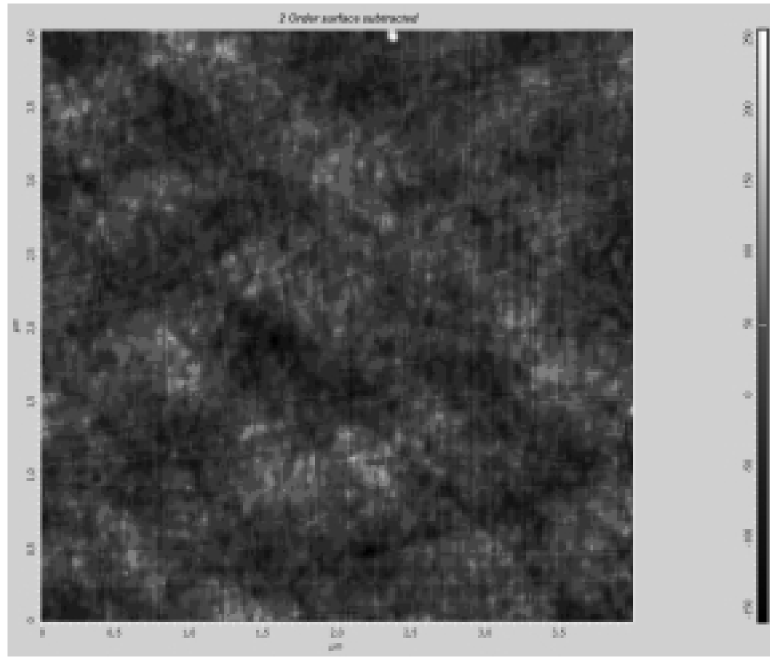

Fig. 6. AFM-image of the surface of a standard sapphire substrate of industrial production (2 dm in diameter) obtained by zonde microscope “Solver P-47 H”. Statistical characteristics of topography of the sapphire substrate surface are as follows: peak-to-peak, *Sy* =0.50944 nm, average roughness, *Sa* =0.0488603 nm, root mean square, *Sq*=0.0602714 nm.

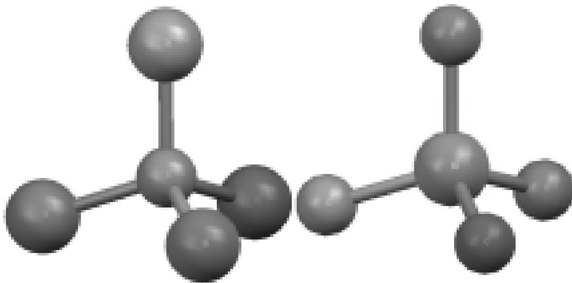

Fig. 7. Main structural elements for all types of SiC. Length of Si-C bond equals to 1.89 Å, whereas, that of Si-Si- and C-C-bonds is equal to 3.08 Å.

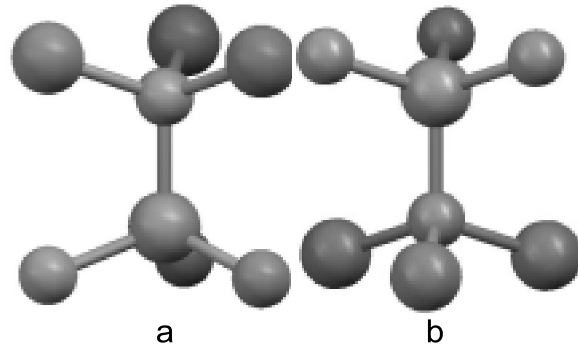

Fig. 8. Arrangement of atoms in hexagonal SiC - a, and cubic SiC -b.

tice mismatch for this pair is 3.1%. In addition, the thermal conductivity coefficient of SiC is high (3.8 Wt/cm K), whereas, doped SiC possesses high electrical conductivity. It implies that electric contacts can be mounted on the reverse side of a substrate, and the technology of device manufacturing is sharply simplified here. There are both polar C-polar substrates of silicon carbide, the so-called C-substrates, and Si-polar substrates, i.e. Si substrates. In the first case, C-atoms go into the substrate surface, whereas in Si substrates just Si-atom passes there. Nowadays, Si-substrates are more preferable, because GaN films grown on them are of top-quality.

The main limitation of silicon carbide lies in its high cost. A high-quality 4 inch wafer costs about 3000 $, whereas wafer of a larger diameter are not available now. Lattice mismatch of 3.1% leads to formation of defects in a marked quantity, and this fact opposes to develop high-current devices. In addition, after the termination of growth process, a need to etch off an initial substrate arises; C this is

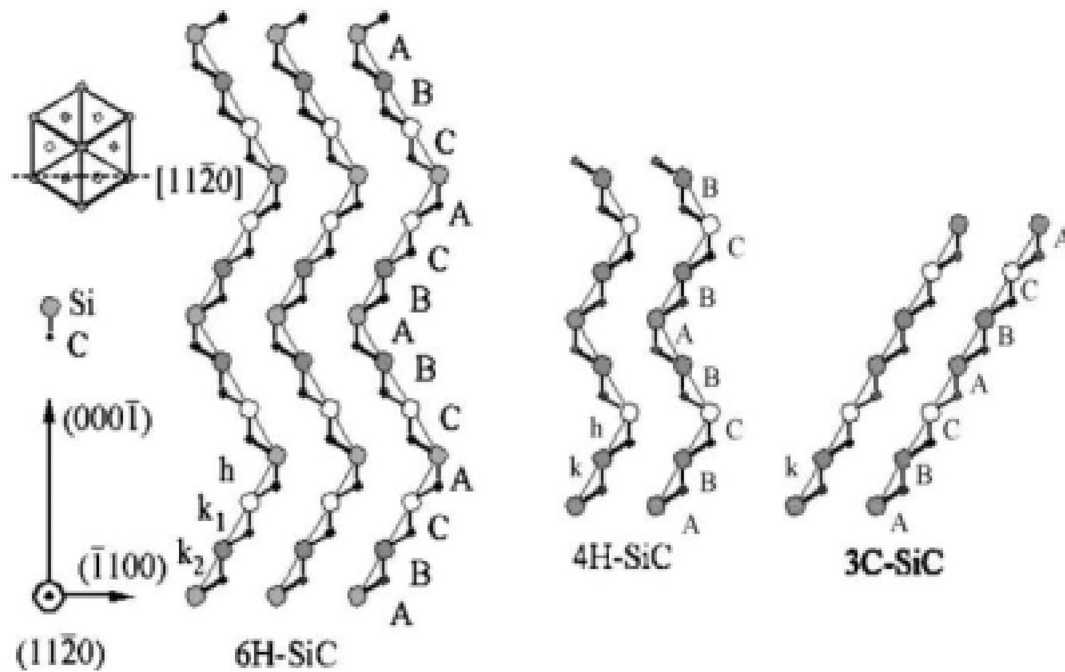

Fig. 9. Close-packed planes A, B, C in different polytypes of SiC.

a hard task in the case of SiC, because etching off the material is a very tedious and complex process.

Silicon carbide exists in more than 250 polytypes, which are characterized by alternation of various tightly-packed biatomic planes [7]. The main element of all the polytypes is a covalent bonded tetrahedron formed of C-atoms and Si-atom centrally located and vice versa a tetrahedron composed of Si-atoms with C-atom centrally positioned, Fig. 7.

As for hexagonal polytypes of SiC, C-atoms of the first tetrahedron are strictly located over Si-atoms of the second tetrahedron, and vice versa (see Fig. 8a), whereas, in a cubic polytype, they are located uniformly between them, i.e. turned by 60^0 (see Fig. 8b).

Various polytypes are differed in the arrangement of tightly-packed biatomic layers of silicon and carbon, which are of the three types, and they are designated as A, B, C [17]. An arbitrary view of successive biatomic A-,B-,C - planes along [11-20]-direction for main polytypes of SiC, such as 6H, 4H, 3C, and 2H, is shown in Fig. 9, whereas Fig. 10 represents a real view of the polytypes along [11-20] - direction [7].

Lattice constant *a*, for all hexagonal types is nearly equal to 3.08 A, whereas *c* is the constant for 2H-, 4H-, and 6H-polytypes amounts to 1.641 A, 3.271 A, and 4.908 A, respectively, and these numbers are approximated to perfect values, namely, $\sqrt{8/3}$, $2\sqrt{8/3}$, $3\sqrt{8/3}$. Hexagonal polytypes are of one and the same $P6_3mc$ - space group, as well as, wurtzite GaN. As for the cubic polytype, it refers to F-43m group. Main structural, physical and mechanical properties of SiC are given in Table 5.

It should be mentioned that only two polytype, 4H and 6H, are commercially available substrates of high-quality. Solid SiC-crystals are produced by sublimation method, i.e. a modificated Lely's technique designed by Tairov and Tcvetkov in 1978. Growth in this case proceeds at temperature 2200 ^{0}C and pressure from 20 to 500 Torr in argon atmosphere. Nowadays, substrates up to 4 inches in diameter with vicinal surface both of silicon and carbon polarity deviated out of [0001] by 3.5^0 for 6H-SiC and 8^0 for 4H-SiC are produced.

A main problem in growing gallium nitride on silicon carbide lies in the fact that SiC is not wetted with gallium nitride. Therefore, as it is taken in practice, a thin buffer AlN-layer as a good wetting agent

Table 5. Basic properties of SiC.

Properties	Polytype	Value
Lattice constant (nm)	3C	a=0.43596
	2H	a=0.30753, c=0.50480
	4H	a=0.30730, c=1.0053
	6H	a=0.30806, c=1.51173
Density (g/cm^3)	3C	3.166
	2H	3.214
	6H	3.211
Melting point (^{o}C)	3C	2793
Heat capacity (J/g K)	6H	0.71
Thermal conductivity (W/cm K)	3C	3.6
	4H	3.7
	6H	4.9
Linear thermal expansion coefficient (10^6 K)	3C	3.9
	6H	4.46 a-axis
		4.16 c-axis
Relative change in lattice constants	3C	$\Delta a/a_0$: 0.4781, $\Delta c/c_0$: 0.4976
(300–1400K)		$\Delta a/a_0$: 0.5140
Young's modulus (GPa)	3C	~440
Poisson's ratio	Ceramic	0.183–0.192
Refractive index (ordinary ray)	3C	2.6916, λ = 498 nm
	2H	2.6686, λ= 500 nm
	4H	2.6980, λ = 98 nm
	6H	2.6894, λ = 498 nm
Energy band gap (eV) (T <5K)	3C	2.4
	4H	3.26
	6H	3.02
Charge carrier mobilities (cm^2/V s) (300K)	3C	800 – electrons, 40 – holes
	4H	1000 – electrons, 115 – holes
	6H	400 – electrons, 101 - holes
High breakdown electric field (V/cm)	3C	$2.12 \cdot 10^6$
	4H	$2.12 \cdot 10^6$
	6H	$2.12 \cdot 10^6$
High saturation drift velocity (cm/s)	3C	
	4H	$2 \cdot 10^7$
	6H	$2 \cdot 10^7$
Static dielectric constant	3C	9.72
	4H	9.65
	6H	9.66
Electrical resistivity (undoped) (Wcm)	3C	
	4H	10^2 - 10^3
	6H	

for SiC, is deposited on the surface of SiC before GaN growing. After this operation, the growth of GaN is carried out in layer-by-layer manner (see Fig. 11).

As in the case with sapphire, there is a great number of different techniques to increase the quality of GaN growth on hexagonal SiC. Large difficul-

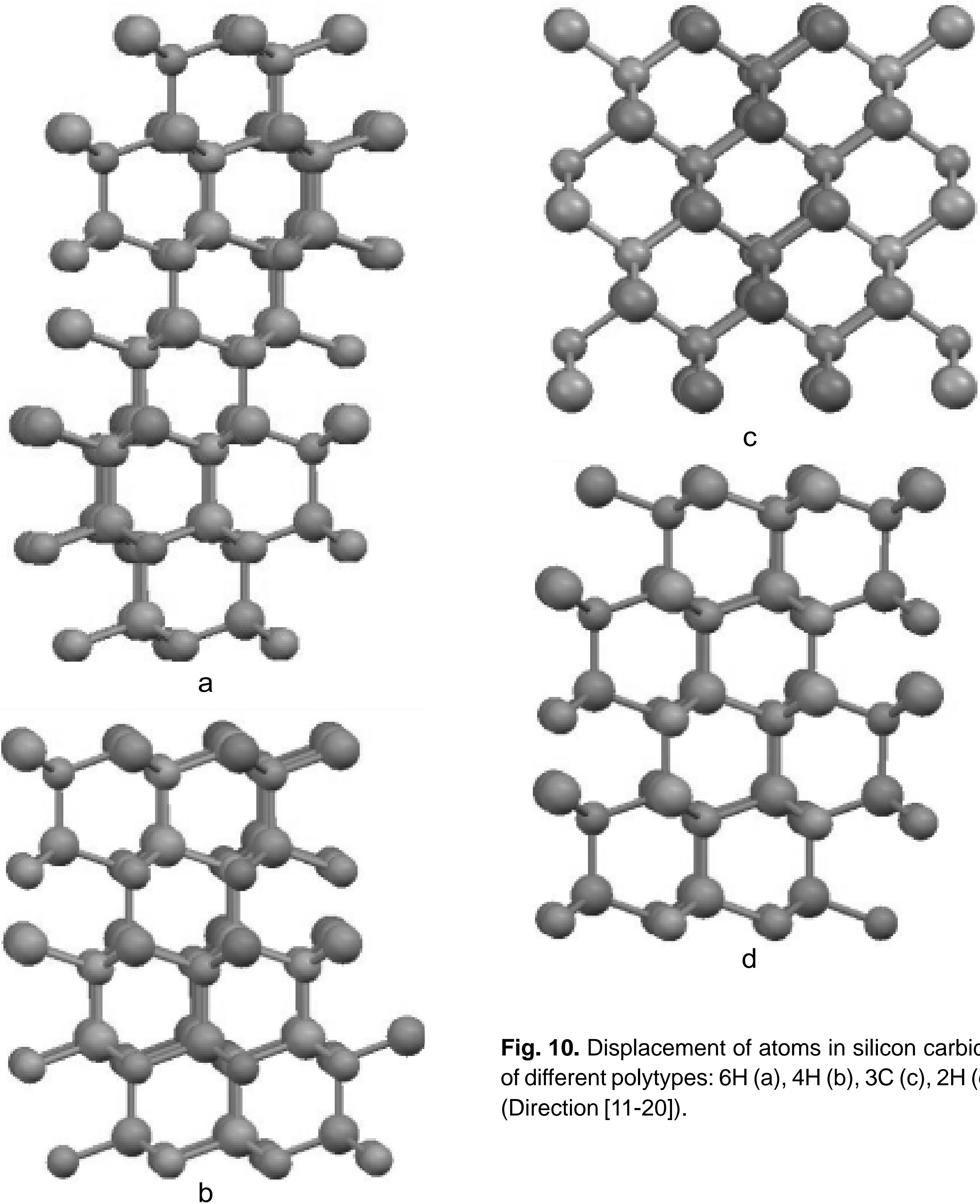

Fig. 10. Displacement of atoms in silicon carbide of different polytypes: 6H (a), 4H (b), 3C (c), 2H (d) (Direction [11-20]).

ties are also originated in the course of SiC-surface treatment due to its roughness.

Fig. 12 demonstrates the images of surfaces of 6H-SiC(0001)-polytype after coating with 0.05 nm of AlN (Fig. 12a) and 4x4 phase of GaN (0001) (Fig. 12b) obtained by scanning tunnel microscope (STM-patterns), see Refs. [18,19].

As for cubic SiC, the cubic GaN-layer was reported to be grown on it [20] in spite of difficulties associated with its stabilization. It was found that an increase in nitrogen concentration led to preparation of a more stable cubic phase. However, quality of a cubic GaN is certainly lower than that of a hexagonal one; the half-width of X-ray rocking curve

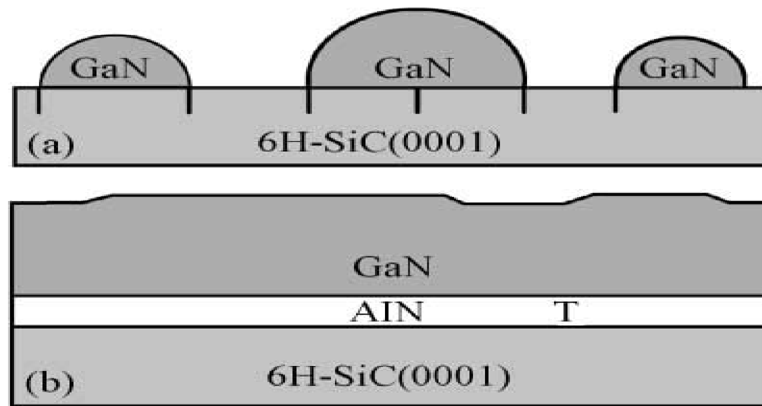

Fig. 11. (a) Schematic of GaN/SiC and (b) GaN/AlN/SiC growth.

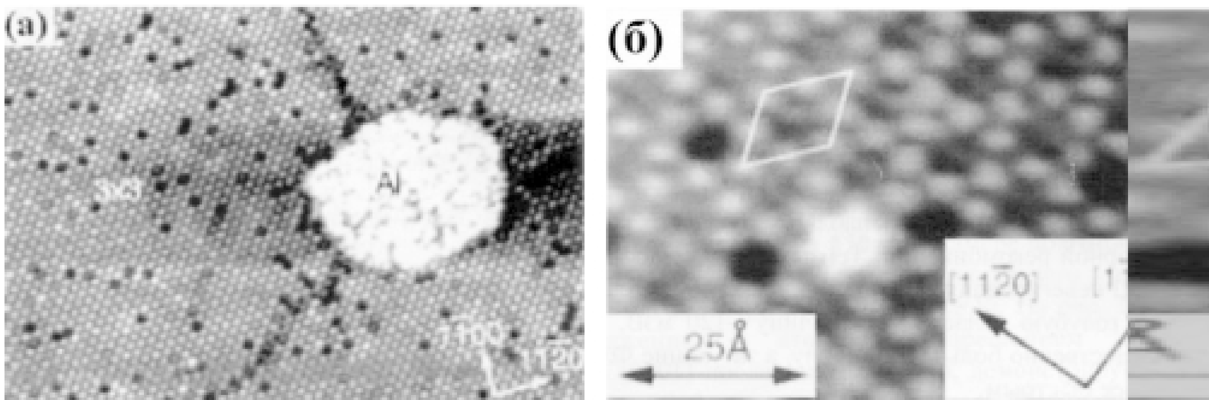

Fig. 12. STM-patterns: (a) – 6H-SiC(0001) – surfaces after coating with 0.05 Al-monolayer at room temperature and annealing at 600 °C; (b) – after coating with by 4x4 phase of GaN(0001) at *Vs*= -2,8 Â [18,19].

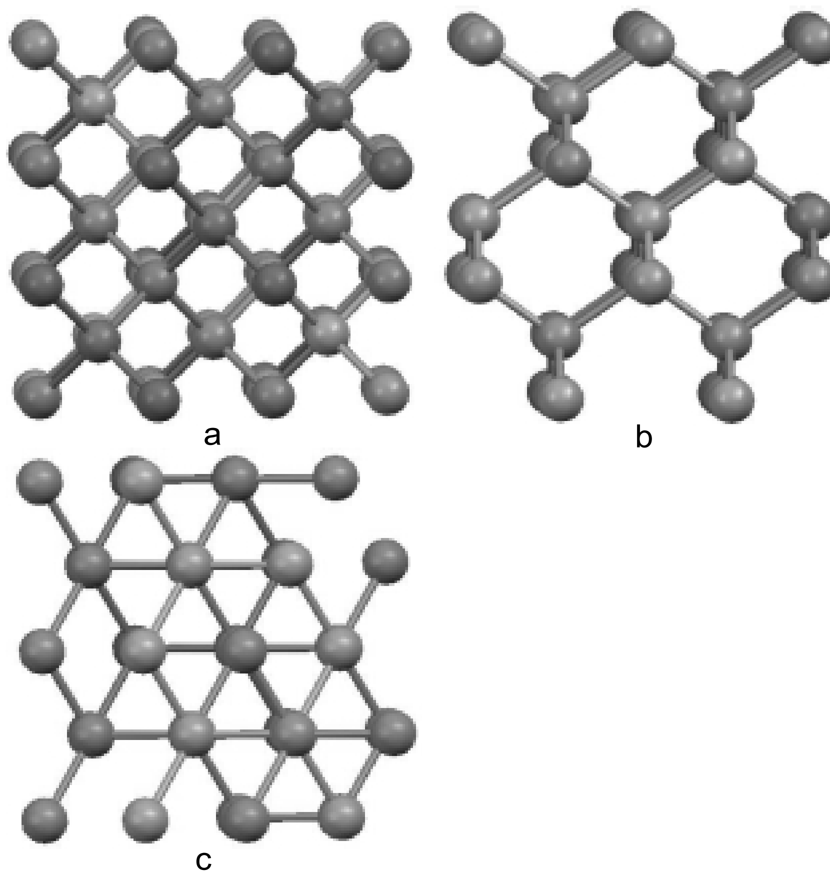

Fig. 13. Perspective view of Si along various directions: (a) [001], (b) [011], (c) [111].

Table 6. Main physico-mechanical properties of silicon.

Properties	Value
Lattice constant (nm)	0.543102
Density (g/cm^3)	2.3290
Melting point (^{o}C)	1414
Heat capacity (J/g K)	0.70
Thermal conductivity (W/cm K)	1.56
Thermal diffusivity (cm^2/s)	0.86
Thermal expansion(linear) 10^6 K	2.616
Relative change in lattice constant: a/a_0 (298–1311K)	0.3995
Shear modulus (GPa)	680
Bulk modulus (GPa)	97.74
Young's modulus (GPa)	165.6
Poisson's ratio	0.218
Refractive index	3.42
Static dielectric constant	11.8
Electrical resistivity (undoped) (kW cm)	Up to 50
Energy band gap (eV)	1.124
Electron mobility (cm^2/V s)	1430–1448
Hole mobility (cm^2/V s)	473–495

equals as a rule 10 arcmin for cubic GaN in comparison with 2 arcmin for hexagonal GaN.

2.4. Silicon

Silicon is the most superior material to use it as a substrate for GaN due to its excellent physical properties, the highest quality, large wafer sizes, and low cost. Si-crystals are the most perfect and smooth; in addition, possibility to integrate optoelectronic devices on GaN-base with Si-microelectronics appears to be very attractive. However, nowadays the quality of GaN-layers grown on Si is noticeably lower to a high degree than in the case with sapphire; first of all, it is due to the mismatch in Si-and GaN lattices and, also, due to the silicon tendency to form amorphous SiN. As a result, both GaN and of AlN films possess low luminescence capacity and they grow on Si with a lot of defects.

Silicon has diamond-like lattice structure with cubic space Fd-3m-group. The Si-lattice can be represented as two inter penetrating face-centered cubic lattices [17]. An image of atomic Si-structure along [001]-, [011]- and [111]- directions is gi-ven in Fig. 13. Main physico-mechanical properties of Si are summarized in Table 6.

Both cubic and hexagonal GaN can be grown on Si(001). As a rule, the film is a combination of cubic and hexagonal types due to formation of amorphous Si_xN_y -layer of a few nanometers in thickness on the interface [21]. In order to avoid this effect, the best way is to apply a thin SiC-layer on Si by CVD-technique. A pure cubic phase of GaN can be prepared in this case. It should be also mentioned that sometimes buffer Al_2O_3, AlN, $Al_xGa_{1-x}N$ layers are also used. However, the films prepared within these approaches are still of low quality.

Si(111) substrates are believed to be more preferable to grow GaN. Since Si is not an isomorphous substrate, the presence of steps on it results in formation of such defects as mismatch packing boundaries. The half-width of X-ray rocking curve for Si equals about 20 arcmin. In order to avoid the formation of an amorphous Si_xN_y layer, buffer SiC, AlN, $Al_xGa_{1-x}N$, AlAs, ZnO and some other layers are applied as well. The best effect has application SiC and AlN.

Unfortunately, the thermal expansion coefficient of Si is more than two times lower as compared to that of GaN, and this results in cracking of GaN-layers of rather high quality at cooling [22]. Appli-

cation of various buffer layers, in particular, AlN, AlO_x, and porous Si-layer is proposed to solve the above problem.

3. III- PLANE NITRIDE STRUCTURES. MAIN TECHNIQUES AND INSTRUMENTION

3.1. Main techniques

As it was mentioned above, heteroepitaxy on foreign substrates is, as a rule, used for the development of the devices based on nitride semiconductors. α-Al_2O_3 sapphire and SiC are the most commonly used materials for heteroepitaxy. Although sapphire is of rhombohedral structure, it can be described by means of hexagonal cell. At present, sapphire of four orientations is used as substrates, where (1010) is the *m*-plane, (0001) is the *c*- plane, (2110) is the α - plane, and (1120) is the *r*-plane (see Fig. 14).

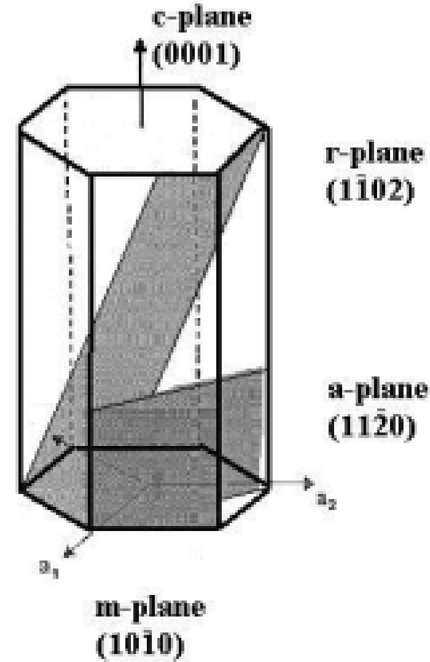

Fig. 14. α -, *m*-, *r*- planes of whurzite crystal represented schematically.

The hexagonal lattice of GaN has principal directed “c”-axis, therefore, symmetry of the crystals allows a built-in polarization along the axis. Deformation of heterostructure due to differences in lattice constants and in thermal expansion coefficients leads to origination of additional polarization associated with a piezo-effect; note that a vector of the polarization might be arbitrarily oriented. In the case where *z*-direction is parallel to “c” or [0001], the polarization can be estimated as

$$P_z = 2\varepsilon\left[e_{zx} - \left(C_{xz} / C_{zz}\right)\right]. \quad (1)$$

at $\varepsilon_{xx} = \varepsilon_{yy} = \varepsilon$ according to the determination the electric field generated is equal to

$$E_z = -P_z / \varepsilon_r \varepsilon_0, \quad (2)$$

where ε_r and ε_0 are the dielectric constants of the semiconductor and in vacuum, respectively.

Under equilibrium conditions, the built-in electric potential of E_z/e – amplitude is screened due to spontaneous generation of electron-hole pairs within the volume of a semiconductors layer. However, the magnitude of a dielectric field may reach 10^6 V due to piezoeffect caused by mechanical stresses, for instance, in InGaN/GaN – heterostructure which is most commonly used in light-emitting diodes [23].

In general, epitaxial GaN-layers are grown on *c*-plane of sapphire. Recently more emphasis is given to the epitaxy on α-, *m*-, and *r*-planes. The main techniques for preparation of GaN- and AlN-epitaxial layers are the following: molecular-beam epitaxy (MBE); chloride gaseous phase epitaxy (HVPE), and metalorganic chemical vapor deposition (MOCVD) where metalorganic compounds are used as precursors.

Crystallization of layers produced by MBE-technique proceeds due to reaction of an atomic flow of Ga with that of N, namely:

$$\mathrm{Ga}(l) + \mathrm{N}(d) = \mathrm{GaN}. \quad (3)$$

An energy of ~ 10 eV is needed to produce atomic nitrogen by N_2 dissociation. In the case, when ammonia is the nitrogen source, the following reaction takes place:

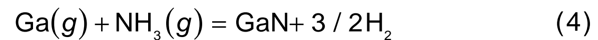

$$\mathrm{Ga}(g) + \mathrm{NH_3}(g) = \mathrm{GaN} + 3/2\mathrm{H_2} \quad (4)$$

As a rule, typical temperatures of GaN and AlN-layers growth are to 960-1040 and 1040-1115 °C, respectively. Analysis of deposition conditions shows that the mechanism of growth on a singular surface is determined by the only parameter that as the ratio of deposition rate to surface diffusion coefficient of adatoms [24,25]. MBE-technique allows to control the distribution of an impurity over a crystal surface by means of selection of a face reorientation angle, as well as the temperature of epitaxy [26].

As for HVPE-technique, it is usually used to form thick GaN-layers (>100 mm); so, such a system is a rather complicated from the point of view of thermodynamics. Strong dependence of GaN formation reaction on hydrogen content in a growing system is described in Ref. [27]. It is shown in the paper that there are three domains in Ga(l)-HCl(g)-NH_3(g)-system at ~ 1000 °C; they are pure GaN, liquid Ga, and mixed area involving GaN and liquid Ga.

We were succeeded in finding essential differences in reaction mechanisms of synthesis both of GaN and of AlN using the data described in Ref. [28]. For purposes of thermodynamic analysis, the growth system was divided into three parts, such as, the zone of Al-source, the zone of Ga-source, and the growth zone. The following chemical reactions were analyzed in the each zone:

Reactions proceeding within the zone of Ga-source

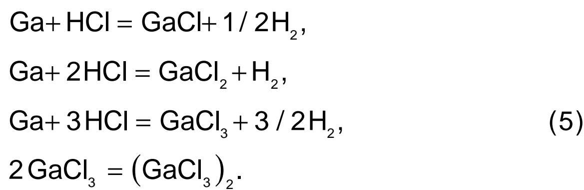

$$\begin{aligned} &Ga + HCl = GaCl + 1/2H_2,\\ &Ga + 2HCl = GaCl_2 + H_2,\\ &Ga + 3HCl = GaCl_3 + 3/2H_2,\\ &2GaCl_3 = (GaCl_3)_2. \end{aligned} \quad (5)$$

Reactions proceeding within the zone of Al-source

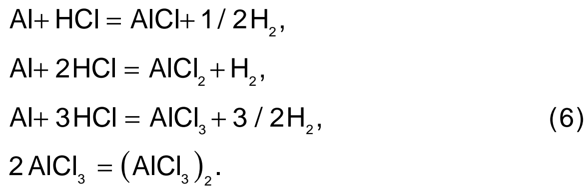

$$\begin{aligned} &Al + HCl = AlCl + 1/2H_2,\\ &Al + 2HCl = AlCl_2 + H_2,\\ &Al + 3HCl = AlCl_3 + 3/2H_2,\\ &2AlCl_3 = (AlCl_3)_2. \end{aligned} \quad (6)$$

Reactions proceeding within the growth zone

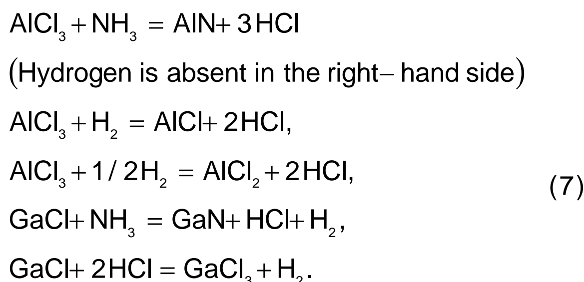

$$\begin{aligned} &AlCl_3 + NH_3 = AlN + 3HCl\\ &(\text{Hydrogen is absent in the right-- hand side})\\ &AlCl_3 + H_2 = AlCl + 2HCl,\\ &AlCl_3 + 1/2H_2 = AlCl_2 + 2HCl,\\ &GaCl + NH_3 = GaN + HCl + H_2,\\ &GaCl + 2HCl = GaCl_3 + H_2. \end{aligned} \quad (7)$$

Decomposition reaction of ammonia

$$NH_3 = (1-\alpha)NH_3 + \alpha/2N_2 + 3\alpha/2H_2. \quad (8)$$

It is worth to note that molecular gaseous hydrogen (H_2) is absent in the right-hand side of reaction of AlN-synthesis, whereas it is formed in GaN synthesis. This fact determines either absence or presence of a strict qualitative dependence of a growing layer on H-content in a gaseous mixture.

So, we noted that synthesis of AlN layer is to be carried out in hydrogen atmosphere. In spite of the fact that the data of thermodynamic analysis do not show great differences in the growth of AlN either in hydrogen, or in an inert gas, it should be mentioned that the attained degree of hydrogen purification is much higher, as compared to that of any other suitable gaseous carrier. This factor is of great importance in preparation of high-quality buffer AlN layers. As for transition to the growth of GaN-layer in inert gas atmosphere, it leads to the sufficient increase in the area of existence of pure GaN, and this gives rise to much more reproducibility of the results in engineering processes, where Ga–HCl–NH_3-system is used. In addition, the factor allows to vary more freely experimental conditions with the aim to obtain mirror-smooth morphology in realization of 2D-growth, along with saving of the high crystalline quality of GaN-layers. Typical temperatures of GaN epitaxy 950-1050 °C and AlN - 1000-1080 °C are given in Fig. 15.

At present, MOCVD method becomes a main technique for growing of epitaxial layers and development of semiconductor devices based on GaN. Reaction of interaction between metalorganic compounds, such as, trimethylaluminium $Al(CH_3)_3$), trimethylgallium $Ga(CH_3)_3$) and ammonia is the basic of this method.

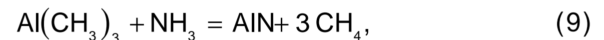

$$Al(CH_3)_3 + NH_3 = AlN + 3CH_4, \quad (9)$$

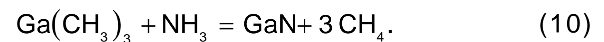

$$Ga(CH_3)_3 + NH_3 = GaN + 3CH_4. \quad (10)$$

In the cases of MOCVD method, the maximal epitaxy temperature is 900-1000 °C.

3.2 Instrumentation based on polar gallium-nitride semiconductors

Nitride semiconductors are very attractive from the point of view to use them in development of optical devices of short-wave range. The first epitaxial GaN-film on a sapphire substrate was grown by a hydride gas-transport epitaxy method in 1969, [29] and in 1971 induced emission of GaN within the UV-range at 2K was demonstrated [30]. In that year the first light-emitting diode of blue glow based on GaN on a metal-dielectric-semiconductor structure MDS was performed [31].

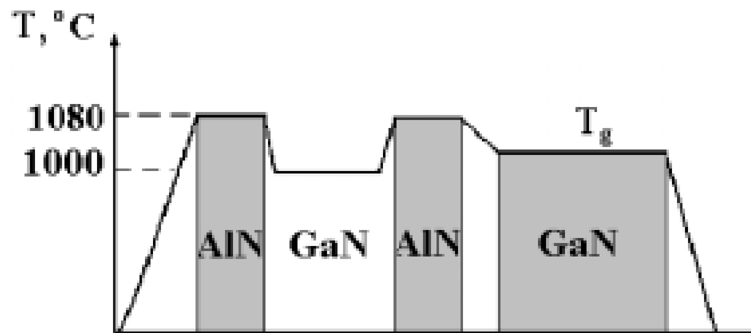

Fig. 15. Time-temperature regime of epitaxy of multi-layer GaN/AlN structures by HVPE, see Ref.[28].

A light-emitting diode of MDS-structure was produced in 1979 (see Ref. [28]); it was based on GaN grown on a structural SiO_2-substrate by the hydride gas-transport technique. In1979 I. Akasaki *et al.*, for the first time, used metalorganic gas transport epitaxy in NH_3-atmosphere at temperatures over 1000K to grow a GaN-film on a sapphire film. However, the final result was negative, i.e. the epitaxial film possessed a lot of defects. This fact was accounted for the difference in surface energies of sapphire and GaN. In order to avoid the difference, the authors decided to use a buffer AlN-layer, which had to be growth at low temperature; it's properties were supposed to be similar with both a substrate and a semiconductor. The experiments were successful and in 1985 the high-quality GaN-film was made [33]. Residual concentration of electrons was equal to 10^{15} cm^{-3} in the new films. Thus, the use of the buffer layer resulted in sufficient increase in the film quality and it led to essential upgrade in luminescent and electronic properties of GaN-films. It should be mentioned that just the same group of researchers in 1990 obtained the induced radiation within UV-range at room temperature that was needed to construct GaN-laser [34].

In order to go to the next stage in application of GaN-structures it was needed to prepare GaN with hole conductivity and to manufacture layers with desired electronic conductivity. As it was noted above, application of a buffer layer led to improvement of the quality and electronic characteristics of a sample. Nevertheless, even addition of such acceptor as Zn did not provide the hole conductivity, because concentration of residual electrons was too high. Only in 1989, attempts to solve the problem met with success. Decrease in concentration of residual electrons was achieved using Mg as an acceptor and electron irradiation of a film during its growth [35]. Necessary control over the electron conductivity of GaN and AlGaN was performed by SiH_4 -doping [36,37]. An essential increase in the external quantum yield of radiation after provision of p-n transition on GaN-film of high quality is to be noted. At present, blue light-emitting diodes based on multi quantum GaInN/GaN –wells possess quantum yield over 35%, and they shine more brightly than filament lamps. It should be mentioned that various defects in concentrations of ~ 10^8-10^{10} cm^{-2} are present in GaN grown even on a buffer layer; however, the defects do not exert great influence on parameters of laser diodes, but useful life of the latter is affected by them. By means of such techniques as micro channel epitaxy and growing on a doped substrate, dislocation concentration was decreased up to 10^7 cm^{-2}. For comparison, we note that in 1997 the useful lifetime of laser diodes was equal to 10000 hours at room temperature and output power of 2 mWt (see Ref. [38], for some time past in 2000 it was increased up to 15000 hours at 60 °C and power of 30 mWt [39]).

Main results obtained in development of instruments based on nitride semiconductors are cited in some reviews [40-43], therefore, we describe only some recent advances made in this field.

Semiconductor compounds of Ga-, Al-, and In-nitrides are used in many fields of science and technique; some of them are described below.

The above-mentioned structures are used in development of lasers of new generation for systems of storage and representation of information, and they are by an order better, relative to the density, as compared to all now-existing ones. Thus,

over all efficiency of blue-violet light-emitting diodes based on AlInGaN. To solve the problem, as a rule, a layer of wide-band gap AlGaN-semiconductors, interlocking electrons in an active current can be left still heavy. In order to suppress flowing of electrons back into the active area, multiple quantum barriers (MQB) AlGaN/GaN or the so-called multiple quantum well structures (MQW) InGaN. The structures were grown on a sapphire substrate by MOCVD-technique using longitudinal overgrowing of layers. To interlock electrons in the active area, in some works, two different layers were used, namely, a single $Al_{0.2}Ga_{0.8}N$:Mg layer of 20 nm in thickness or MQB layer $Al_{0.2}Ga_{0.8}N$/GaN of the same thickness as that of the former. Note that the authors succeeded in decreasing of threshold generation current from 42 to 32 mA at room temperature and in increasing in the slope of watt-ampere characteristics from 0.90 to 1.12 Wt/A by means of involving the layers described above.

Further, the above-mentioned semiconductor GaN-compounds are used in economical lighting units of lasting quality, which are in maximum agreement with natural illumination according to their spectra. Active usage of the solid lighting devices promises real revolution in the energy power saving and ecology. In development of powerful emitting diodes of green, blue, ultraviolet, and while glow, the quantum structures based on GaN, such as, InGaN/GaN, are very promising. In this connection, the problem of improvement of their efficiency, which depends on an inner quantum output and coefficient of rational removal, is a very actual one. As for the inner quantum efficiency, nonradiative recombination processes along with heavy piezoelectric fields induced by mismatch in lattice constants of radiation removal, in its turn, decreases due to processes of the total inner reflection and supersaturation of radiation in the GaN-layer. In order to increase the coefficient of radiation removal, different technologies are used such as formation of a textured Al_2O_3 substrate, providing of rough surfaces within p-GaN: Mg- and n-GaN-Si-areas, longitudinal overgrowing on nonpolar GaN layers and some others. A rough surface obtained over an active layer with multiple quantum wells can, largely, increase both the inner output and coefficient of radiation removal. Structures with the following layers were grown by MOCVD-technique: the intentionally undoped n-GaN layer with a thickness of 1 μm; n-GaN layer (3 μm); the active layer included 19 pairs of multiple quantum InGaN/GaN wells followed by p-GaN layer doped with magnesium. Active layers consisted of InGaN well (30 Å in thickness) and GaN barrier (70 Å). After creation of porous p-GaN structure, photoluminescence spectra showed a pronounced increase in radiation intensity; in addition, the phenomenon of a shift of radiation maximum by 9.5 nm (56 meV) in the blue area was noticed for the structure. The shift originated due to partial removal of mechanical strains in the structure and, accordingly, due to a decrease in piezoelectric fields (note that an estimation of piezoelectric field attenuation amounted to ~0.2 MW/cm), Ref. [45]. This year low cost AlGaN/InGaN/AlGaN – emitting diodes having radiation maximum of 415 nm and radiation spectrum half-width (FWHM) equal to 0.37 eV were prepared by HVPE-technique for commercial usage [46]. Whereas light-emitting diodes based on AlGaN radiating in a deep UV region of spectrum (300 nm) were grown on solid AlN substrates by MOCVD technique [47].

Furthermore, the above described compounds are used in constructing of high temperature, high speed devices and integrators. Recently high-electron mobility transistors (HEMT) based on AlGaN/GaN heterostructures demonstrate perfect characteristics. Nevertheless, the authors of Ref. [49] succeeded in obtaining of aluminium nitride of n- and p types. Varying the dislocation concentration, diminishing and precise controlling the doping level, the authors of [49] managed to raise the mobility of charge carriers at room temperature. Namely, they obtained such concentration of electrons as $7.3 \cdot 10^{14}$ cm^{-3} and the record mobility of 426 cm^2 Å^{-1}s^{-1} (at 300K) at Si concentration of $3.5 \cdot 10^{17}$ cm^{-3} (data from Hall effect measurements). The electroluminescence efficiency of a light emitting diode was increased up to 70 times in the presence of AlN layer and supperlattice of p-type. The output radiation power was 0.02 μWt under 40 mA current at the wavelength of 210 nm.

As an alternative, the mentioned structures can be also used in development of acoustic wave devices due to the fact that GaN crystals are characterized by high piezoelectric constant.

In conclusion, it is to be said that the materials described above may function as near-infrared sources on GaN, for instance, in devices of night-glow vision, chemical and biological sensors, optico-telecommunication systems, *etc.* Such sources are conventionally fabricated on AlGaAs and InGaAsP semiconductor materials; nevertheless, the above semiconductor compounds have an essential drawback, which consist in strong temperature dependence of output characteristics. However, it should be mentioned that, at present,

an interest to the sources based on GaN doped with rare earth ions is noticed. GaN has a series of advantages for initiation of IR radiation as compared to other materials since this compound represents a direct gap and wide bandgap semiconductor of high chemical and thermal stability and it can be doped with rare earth compounds up to high concentration. In most works, thallium (Tm), neodymium (Nd), and erbium (Er) are chosen for doping. Moreover, the radiation is observed at temperatures up to 550 °C.

Note that, as a rule, the above-described units are made as thin-film, multilayer structures such as a metal-semiconductor-isolator-metal of 250 nm Al, 500 nm GaN, 200 nm Al_2O_3-TiO_2, 300 nm indium-stannum oxide on Si-substrate. Up to date, for GaN doped Tm, Nd, and Er, the output electroluminescence efficiency of $1 \cdot 10^{-6}$, $1 \cdot 10^{-5}$, and $4 \cdot 10^{-6}$, respectively, was attained under the voltage of 4 V [51].

3.3. Structures and devices based on non-polar GaN

As a rule, electronic devices described above are manufactured on the of GaN-structures grown in [0001] direction, which is in parallel to ***c***-axis of wurtzite GaN-crystal. However, using of quantum-dimensional structures in III-nitride optoelectronic devices leads to origination of polarization [52]. In order to manufacture non-polar GaN, structures either on sapphire substrates with output on **r**-plane (see Refs. [53-59]), SiC-substrates with output on m-SiC plane or another type substrates, for instance, lithium aluminates (γ-$LiAlO_2$, see Refs [60,61]) are used. Preparation of non-polar quantum-dimensional AlGaN/GaN (see [53]) and InGaN/GaN (see [54]) – structures by MOCVD- and HVPE-techniques is described in papers [49-61].

Starting from the abovementioned assumptions, possibility to make laser diodes based on m-plane of InGaN/GaN under threshold voltage of 6.7 eV and current density of 3.7 kA/cm^2 (see Ref. [62]) as well as current density of 7.5 kA/cm^2 (see Ref. [63]) was demonstrated. Bright light-emitting diodes were based on m-plane on InGaN MQW –structure, where maximum of emission peak and quantum efficiency were equal to 468 nm and 16.8%, respectively. Emissive power of the structures amounted to 8.9 mW at current of 20 mA [64]. Non-polar α-plane GaN-layers were grown on Si(100)-substrate by a laser deposition technique using a buffer MnS(100)-layer of GaN[1100]/MnS[010]/Si[010] configuration [65]. The above-cited result opens silicon nitride structures.

4. GaN/Si STRUCTURES. BASIC METHODS AND DEVICES

4.1. Problems in fabrication of the structures on silicon

Devices in gallium nitride electronics are usually manufactured on sapphire or silicon carbide substrates. However, high price of SiC substrates and low conductivity of sapphire ones compose a serious obstacle to fabrication of GaN based apparatus. As for silicon substrates, they have high conductivity, large sizes, and low price, and, therefore, at present, such materials draw attention of investigators with the aim to use them in gallium nitride electronics.

There is a large difference in lattice constants (17%) and thermal expansion coefficients (33%) between GaN and Si; that leads to formation of substantial deformations in an epitaxial layer, high density of defects of different nature, and cracks in epitaxial layers grown directly on silicon. In addition, a capability of silicon to react with ammonia at growth temperatures results in significant doping of a layer by donors and, in such a way, formation of p-GaN is hindered [66].

There are a few approaches to overcome above-mentioned difficulties in formation of GaN/Si structures. They are following

Nitridization of the surface. Nitridization of a surface, namely, deposition of an ultra thin SiN_δ layer, is used in growing of GaN on Si -substrates by means of short-time and high-temperature processing of a surface in ammonia flow. It is shown that application of a few intermediate SiN_δ layers can lead to the significant decrease in dislocation density of GaN epitaxial layer on 6H-SiC-substrate [67]. Preliminary deposition of few Al monolayers leads to a decrease of a nitridization barrier [68], whereas formation of an ultra thin buffer layer of AlN after nitridization results in the improvement of the surface quality of subsequent GaN layer [69]. For instance, the preliminary deposition of an ultra thin AlN-layer during the GaN on SiC growth leads to similar results [70].

Application of intermediate layers. Various intermediate layers preliminary deposed on a Si-substrate were used to suppress a crack formation process and to decrease the deformation level of epitaxial GaN-layers. In the case of GaN epitaxy on Si, HfN as the buffer layer was formed by

MBE-technique [71], ZrB_2 as the buffer layer was manufactured by MOCVD [72], whereas in preparation of GaN by magnetron sputtering, a buffer ZnO-layer was used [73]. It was shown that in the technology of fabrication of buffer layers by MOCVD method gives rise to crack-free GaN on Si(III) of 1 μm in thickness [74]; whereas application of GaAlN as buffer layers resulted in the increase of crack-free GaN layers thickness up to 2 μm [75]. However, it was shown that the increase in the buffer layer thickness leads to a decrease in the quality of a basic layer; for this reason a technique of buffer layer growth involving a combination of thin AlN and GaN layers was elaborated [76]. In the attempt to grow GaN epitaxial layers on silicon combining of MBE method with thermal treatment in NH_3 flow it appeared that application of a structure consisted of thin AlGaN and AlN layers with layer thicknesses of 120 nm and 250 nm, respectively, was more preferable in fabrication of the crack-free layers [77].

Carbonization of Si-surface. To suppress a crack formation process, it is more preferable to use SiC - layers, since the difference between lattice parameters of SiC and GaN is rather low (3%). Authors of [78] formed a super thin SiC layer on silicon by surface carbonization and then a GaN-layer was grown on it by MOCVD technique; it was shown that the desired parameter of SiC-layer in this approach is the FWHM of X-ray diffraction ~ 360 arcsec, i.e. it should be very close to that of GaN (0002). Note that recently the following procedure was used to produce a perfect crack-free GaN layer of 3 μm on silicon – first, a rather thick (1 μm) 3C-SiC layer was grown on a Si-substrate by chemical reaction of propane and silane (CVD-method); next, a thin AlN layer (50 nm) was formed on it and then the growth of GaN was performed [79].

Application of a superlattice with the aim to decrease the dislocation density. In the case when a large quantity of thin GaN-layers are used as the buffer layer and AlN-layer acts as a "superlattice", the density of dislocations decreases in an order of magnitude [80].

4.2. Deformation of GaN/Si stucture and formation of cracks

Epitaxial growth of GaN on a Si-substrate leads to formation of cracks due to substantial elastic strains initiated due to large scattering in lattice constants and thermal expansion coefficients of GaN and Si. Experimental data show that, as a rule, cracks originate in GaN/Si structures with a thickness of more than ~1 μm [81]. Theoretical estimations show that tangential strains in epitaxial GaN layers grown on Si(111) σ_{xx} ought to result in formation of cracks in the cases, where the thickness of a layer is higher than critical value h_{crit} [82] namely

$$h_{crit} = \Gamma E^* / Z\sigma^2. \tag{11}$$

Here $E^*=E/(1-\nu^2)$, E - is the Young's modulus, ν - is the Poisson's ratio (ν =0.18 [83]), γ - is the surface energy of GaN (γ =1.97 [84]) , Z = 1.976 for a homogeneous layer of GaN, $\Gamma = 2\gamma$ - is the parameter of layer resistivity determined by the hardness value. Note that the hardness value for GaN is equal to 12 GPa, for Si it is 9 GPa, and for SiC - 33 GPa [85].

Estimation of h_{crit} value for GaN/AlN/Si structure shows that the critical thickness of a layer equals to ~ 250 nm for GaN grown on Si in the case when a buffer AlN-layer of 100 nm in thickness is used [86]. Estimation of h_{crit} value for GaN/Si structure with a gradient buffer AlGaN-layer shows that it is increased up to 1 μm here [87].

It should be mentioned that strains originated at cooling of a heterostructure do not lead, as a rule, to formation of new cracks [86]. Actually, estimation of strains induced due to the difference in thermal expansion coefficients of GaN and Si under cooling of GaN/Si-heterostructure from the epitaxy temperature of ~1000 °C down to room temperature showed that the value of thermal elastic strains amounted to $\sigma\sigma_{\Delta\alpha}$ = 0.45 GPa for GaN/Si structure with the thickness of a GaN layer equaled of 15 nm and that of a substrate - 500 nm [87].

Experimental estimates of the value of elastic strains made by the Raman spectroscopy technique showed that the magnitude of residual stains equals to ~0.4 GPa. Therefore, we can conclude that residual elastic strains in a GaN-layer grown on Si are thermal strains induced due to cooling of the structure from the epitaxy down to room temperature. It should be mentioned that the thermal strains may lead to bending of a structure in the case when the thickness of an epitaxial layer is sufficiently large as compared to that of a Si-substrate.

Formation of cracks in epitaxial growth of GaN-layer on Si-substrate with an intermediate buffer AlN-layer takes place due to the difference in lattice constants of layers at the epitaxy temperature. Therefore, maintenance of such conditions for growth of a GaN-layer that cracks should be formed in a buffer layer is one of effective techniques to decrease of cracks into an epitaxial layer.

Since the values of hardness and resistivity for GaN are lower than those for AlN, such conditions can be provided by means of growing AlN- and GaN-layers of different thicknesses; in this case, the removal of strains would occur only in buffer GaN-layers after the AlN-layers had been already grown.

Thus, one of probable ways to suppress origination of cracks in the main GaN-layer is the growth of alternating thin AlN/GaN-layers of thicknesses near critical one (i.e. h_{crit}); in this case, the thickness relation, h_{AlN}/h_{GaN} should be selected regarding for the differences in hardness and resistivity between AlN and GaN.

Another possible ways to suppress crack formation and to decrease the defect concentration in a layer involve application of the epitaxial lateral overgrowth technology on a surface previously modified by a photolithography method [88], a pendeo epitaxy technique [89], and patterned Si substrate method [90]. The authors of [90] show that in growing of a GaN-layer on a Si-substrate, when terraces of sizes from 17 up to 120 nm are used, the quality of GaN upgrades in the same way as in the case with the gallium nitride epitaxy on a sapphire substrate.

4.3 Pecularities of technology for gan growing on Si

Development of technology for growing crack-free GaN-layer on Si-substrate still remains the main problem. With this aim in view, investigators attempt to create elastically deformed but crack free structures and devices based on them. Elastically deformed structures are grown by metalorganic chemical vapor deposition (MOCVD) and molecular-beam epitaxy (MBE) methods. The second problem still unsolved involves preparation of thick layers (>10 μm in thickness) of high quality. In this direction, attempts are undertaken to remove, firstly, strains on a heteroboundary with a Si-substrate and, just after, to remote the working region of a device out of the heteroboundary growing a thick (>100 μm) GaN-layer over the deformation. Stress level in a layer may be reduced applying combinations of different kinds of thick intermediate layers such as GaN or AlN. For this aim, rather thick layers are needed. As for thick layers, they can be grown by the method of gas phase chloride epitaxy, so-called HVPE-technique, which is successfully used in preparation of quasi-volumetric material on sapphire substrates. Therefore, it can be believed that application of Si-substrate instead of sapphire one is promising, since in this case the process of initial substrate removal is sufficiently simplified as compared to that used for sapphire substrates. However, up to date we could not prepare the high-quality thick GaN-layers on a Si-substrate. Comparison of FWHM (the half-width of X-ray diffraction band), ω_{θ}, for GaN prepared by different techniques (see Table 7) allows to claim that layers with a low thickness (~ 5 μm) and HVPE-prepared (15-20 μm) are close to that obtained using carbonized of Si-surface.

It is well-known that the quantity of defects in epitaxial GaN-layers on a sapphire substrate decreases due to increasing of layer thickness; for instance, in the case with growth of GaN-layer on a sapphire substrate, the quantity of defects decreases by the order of 3 in the case of thickness increase up to 60 μm from that of an interface [99]. Therefore, it can be assumed that the relationship is valid for epitaxial GaN-layers on Si-substrates as well.

4.4. Devices based on iii nitride layers on a si-substrate

As present, a few types of devices based on GaN/Si structures are used.

Transistors

As it is known, GaN draws attention to it in fabrication of field transistors due to high values of the electron saturation rate and reverse breakdown in the structure. The thermal conductivity value of a substrate plays a key part for power transistors. Among three basic substrates, such as SiC, sapphire, and Si, which are used to manufacture transistor constructions, SiC possesses the highest thermal conductivity (above 3 W/cm K), whereas Si gives way to SiC, namely, its thermal conductivity is of 1.5 W/cm K. However, Si-substrate is more favorable in fabrication of low cost transistors. As usual, undoped GaN-layers on a Si-substrate are characterized by concentration of secondary charge carriers, which is rather lower as compared to that of GaN-layers prepared on a sapphire substrate. It is due to the fact that after fast nitridization of Si-surface, only a small interface region of GaN-layers is doped with Si, whereas in the case with epitaxy on sapphire (Al_2O_3), oxygen of the substrate penetrates into GaN-layers in a rather large quantity. The first power GaN-transistor on a Si-substrate was presented by "NITRONEX, Inc." company; the transistor parameters were 3.3 W/mm at 2 GHz

Table 7. Comparison of GaN/Si prepared by different techniques.

Growth method	Structure	ω_θ, arcmin	Thickness of GaN-layer	FWHM, arcmin	Dislocation density, cm^{-2}	Reference
NH_3-GSMBE	GaN/AlN/ GaN/Si(111)	15	~1 μm			[91]
RF-MBE	GaN/3C-SiC/ Si(001)		< 220 nm	238		[92]
RF-MBE carboni-zation	GaN/SiC/ Si(111)		20 nm	109 (77K)		[93]
ZnO-RF-sputtering GaN-MOCVD	GaN/ZnO/ Si(001)	13.2				[73]
MOCVD	GaN/ InAlGaN/Si(111)	18	~1			[74]
MOCVD	GaN/AlN/ GaN/Si(111)	~ 6	5.4 μm			[94]
MOCVD	GaN/HT-AlN/ LT-AlN/Si(111)	~7	2 μm			[95]
HVPE	GaN/AlN/ Si(111)	~7	15-20 μm	48 (77K)	$3 \cdot 10^8$	[96]
HVPE/MBE	GaN/AlN/ Si(111)	13.7		64 (50K)	$9 \cdot 10^9$	[97]
MOCVD	GaN/AlN/GaN/ Si_3N_4/Si(111)			60 (300K)	$5 \cdot 10^9$	[98]
SiC-carbo-nization GaN-MOCVD	GaN/SiC/ Si(111)	6-9	~2 μm	144 (300K)		[99]

[100]. HEMTs were made by MOCVD technique on Si (III) substrates of 4 inches in size, and buffer AlN layers and AlN/GaN superlattice were used [101] in their preparation.

Gaseous chemical sensors

GaN polarization and large deformations influence on formation of 2D electron hole gas in AlGaN/GaN/ Si-structure. Even without modulated doping, the density of electrons grown by MBE technique in the 2D channel comes up to the value of $4 \cdot 10^{12}$ cm^{-2}, whereas their mobility amounts to 1620 cm^2/ Vc at room temperature [102]. Due to adsorption of hydrogen and oxygen atoms on the surface of transistors, a volumetric charge layer on the transistor surface is changed along with a change in the conductivity of a channel. Therefore, transistors based on AlGaN/GaN/Si-structures can operate as high-temperature gas sensors [103]. Adsorption effect of molecular gas on an interface layer of the volumetric charge allows to construct more precise sensors based on Pd-AlN/Si structures for registration of hydrogen concentration in air [104].

Light-emitting diodes

Scope for preparation of light-emitting diodes based on GaN/Si structures by MBE method was demonstrated for the first time in 1998 [105]; then blue light-emitting diodes based on InGaN/GaN on Si(III) were made by MOCVD method [106]. Quite recently, the authors of [107] succeeded in growing of high-quality light-emitting diode based on InGaN/ GaN by MQW-technique. The structure with the thickness of about 5 μm without cracks was growth on 150 mm Si(111) (FWHM GaN (0002) is 380 arcsec) at a high degree of homogeneity over the

surface (< 1.1 %) [108]. According to Ref. [109], a possibility to make light-emitting diodes based on InGaN/GaN at radiation maximum in the blue region of the spectrum (455 nm) on Si(001) substrate was shown.

Photodetectors for registration of ultraviolet radiation

High condctivity of a silicon substrate draws attention of researchers to construct UV-photodetectors based on surface-barrier GaN/Si-structures. The first attempts to make UV-photodetectors based on metal-semiconductor-metal structures (SMS) were acquired through preparation of GaN-layers by a reactive evaporation technique [110]. Photodetectors based on Pt-CaN/Si(III) Shottky diode were intended for registration of UV - radiation and they had the sensitivity peak of 0.097 A/W laid within the range of 300 nm [111]. Later the photodetectors with the sensitivity peak of 4600 A/W in the range of 366 nm were manufactured [112].

5. SiC/Si STRUCTURES. NEW APPROACHES TO PREPARATION OF LAYERS OF LOW-DEFECT CONTENT

It would be ideal for GaN-technologies to grow the material on silicon due to unique properties of Si, its cost and capacity to integrate into silicon electronics. However, the misfit between Si and GaN lattices results in high concentration of mismatch dislocations, which is so high that a necessity arises to use sapphire substrates, in spite of a number of negative features typical for structures grown on sapphire wafers. As for silicon carbide, this material provides the highest quality of the structure produced, but its cost is too high and, therefore, SiC is thought to be prohibitive for use in industry. So, at present, active search of new materials for preparation of substrates in GaN-technologies and new techniques to grow GaN-layers of low-defect content takes place. “Pendeo” approach, briefly discussed above, provides low density of dislocations only within a very small section of a substrate (~0.05 mm), and, therefore, it cannot be used for industrial purposes.

In principle, a new approach to the growth of gallium nitride was developed in 2005, where advantages the both Si or SiC and “Pendeo” technique were combined. The main idea of the approach can be summarized as follows. At the first stage, due to chemical etching, pores and etch-pits are formed on the Si-surface. Then, the pores are coated by a thin SiC-layer (~50-100 nm). In accordance with the main concept of “Pendeo” approach, the layer is ideally spread over a porous surface, because the rate of a lateral SiC growth is by an order higher than the rate of vertical growth [10,11,107,108]. Such pores provide optimum relaxation of elastic strains and, in this case, misfit dislocations are not formed, as opposed to traditional techniques discussed above. Details of the process are described in papers [113,114] and patents [115,116]. Refs. [113,114] are more thoroughly discussed below.

5.1. Theoretical substantiation of SiC-coating on Si

In most cases, it is of common practice to deposit SiC on Si by one of three techniques, namely, sublimation in vacuum, molecular-beam epitaxy or chemical precipitation from a gaseous phase. Each of the above techniques has both merits and demerits, however, so far, preparation of a high-quality heteroepitaxial SiC on Si layer by any of the above-mentioned methods failed. First, this is associated with an extremely low density of saturated vapor both of carbon and of silicon carbide at the Si-melting point and below. Therefore, the materials become instantly condensed, and the condensation leads to their low mobility on a substrate surface and, as a consequence, to poor epitaxy. Thus, to improve the quality of epitaxy it is necessary to increase the mobility of material from which the film is grown. As for SiC, this means, that a film is to be grown from a material with high density of saturated vapor over such as of a host crystal, and the material ought to have low bond energy relative to Si. As it is known, that silicon carbide at sublimation is decomposed into a series of compounds, such as SiC, Si, Si_2C, SiC_2. The equilibrium vapor density of gaseous Si and SiC over solid SiC is extremely low at temperatures below 1400 °C. As for the equilibrium vapor density of two other compounds - Si_2C and SiC_2 SiC at T = 1400 °C, although it is by nearly 5 orders of magnitude greater than that of SiC, such property of the two compounds is yet deficient for the marked growth of SiC on Si. So, the idea of SiC deposition under non-equilibrium conditions in the cases, where the density of vapor, supplying a material of higher mobility on Si, is by many order greater as compared to the vapor density that is in equilibrium with solid SiC at deposition temperature, was arised. Among all compounds of Si and C, silicon,

itself, is the only substance, which is in equilibrium with a solid at temperature $T < 1400\ ^{o}$C. Thus, only by means of it, a chemical reaction can be shifted in such a way that concentration of a reaction product ought to become much more than that of an equilibrium one. It should be mentioned that, in the presence of gaseous-excess, the reaction of SiC dissociation on gaseous Si, as well as reaction of SiC_2 formation, should be suppressed in accordance with the Le Chatelier principle; the addition of gaseous Si to solid C leads to gaseous Si_2C as a predominant gas phase component. Thus, gaseous Si essentially increases concentration of a gaseous reaction product only in such a case:

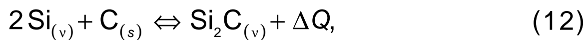

$$2\,Si_{(v)} + C_{(s)} \Leftrightarrow Si_2C_{(v)} + \Delta Q, \qquad (12)$$

where ΔQ is the heat of Si_2C formation. Increasing of concentration of the reagent [Si], for instance, due to evaporation of Si from a substrate displaces the chemical reaction (12) to the right, and this, in its turn, leads to increase in concentration of the reaction product, [Si_2C]. As it follows from Eq. (12), concentration [Si_2C] in this case is proportional to [Si] – concentration squared, i.e. $[Si_2C] = K\,[Si]^2$, where K is the equilibrium constant of chemical reaction (12). The reaction is a very efficient one for transition of SiC growth material due to the fact that heat is evolved in high quantity in the reaction of Si_2C formation. Thermochemical estimations show, for instance, that $\Delta Q \approx 360$ kJ/mol at $T = 1250\ ^{o}$C. With the aim of comparison, we point out that the heat of Si_2C formation in the reaction $Si_{(v)} + SiC_{(s)} \Leftrightarrow Si_2C_{(v)} + \Delta Q$ is of negative sign; it equals to $\Delta Q = -160$ kJ/mol at T=1250 ^{o}C. This provides [Si_2C] concentration nearly 7 orders lower as compared with [Si] concentration in reaction (12), where the concentration is in equilibrium with solid at the same temperature. As for [SiC_2] concentration being in equilibrium in with $Si_{(v)} + 2C_{(s)} \Leftrightarrow SiC_{2(v)}$ - 167 kJ/mol reaction, it is nearly by 4 order lower in comparison with [Si_2C] concentration in reaction (12).

Now we evaluate the value of non-equilibrium Si_2C flow on a substrate. Let p is the pressure of Si_2C formed as a result of chemical reaction (12), where gaseous Si-reagent is in equilibrium with solid Si, i.e. the pressure of its vapor is equal to the equilibrium pressure, p_e. Then,

$$p = K\frac{p_e^2}{p_0}, \qquad (13)$$

where p_0=1 atm is the pressure in its basic state, as it is taken in chemical cal-culations. The equilibrium constant of chemical reaction (12), in this case, is equal to

$$K = \exp\frac{T\Delta S - \Delta H}{RT}, \qquad (14)$$

where R is universal gaseous constant; ΔS and ΔH are the changes in entropy and enthalpy of the reaction process, respectively. In calculating ΔS and ΔH by means of reference data, we get at T = 1250 °C, $T\Delta S$ = -153 kJ/mol, ΔH = -360 kJ/mol, K = $1.3 \cdot 10^7$. Hence, the estimation for pressure of Si_2C: p = 15 Pa follows from Eq. (13). Si_2C in a solid state is absent, therefore, it can not be condensed, and the energy of its bond with Si is well below than that of C or SiC. So, Si_2C molecules on a substrate can attain the following value:

$$J = \frac{p}{\sqrt{2\pi m k_B T}}, \qquad (15)$$

where m is the mass of Si_2C-molecules; k_B is the Boltzmann constant. Thus, we have $J = 5 \cdot 10^{20}$ cm^{-2}s^{-1} at p = 15 Pa and T =1250 °C. The flow of molecules in this case is a rather large one, which, even at a small lifetime, provides the presence of relatively a dense Si_2C adsorbate on the substrate, where the following reaction of decomposition proceeds:

$$Si_2C_{(v)} \Leftrightarrow SiC_{(v)} + Si_{(v)}. \qquad (16)$$

All at once, the gaseous SiC flow formed is added to the solid phase or it becomes decomposed, because the density of its vapor is negligible. As for Si formed, it either incorporates into the lattice of a substrate or evaporates. It should be noted that solid Si and SiC serve as reliable catalysts of the decomposition reaction (16).

For realization of the deposition mechanism proposed, it is needed elsewhere to accumulate silicon, which takes part in reaction (12). Now we describe application of the method in accordance with our patent. A grinded and polished sample of porous carbide, ~ 3 μm in thickness, and of the same diameter as that of a substrate is made by the technique described in [113], and then, it is applied to a Si(111)-substrate with a porous layer apart ~ 1-10 mm. Further, the system is placed into a vacuum heat-treatment furnace, where it is kept during 5-60 min at 1100-1400 °C under a pressure of ~ 10 Pa. At the beginning, Si is evaporated off the substrate surface and it enters porous Si, which absorbs the former like as “a sponge”. The depth of penetration of Si into porous C equals

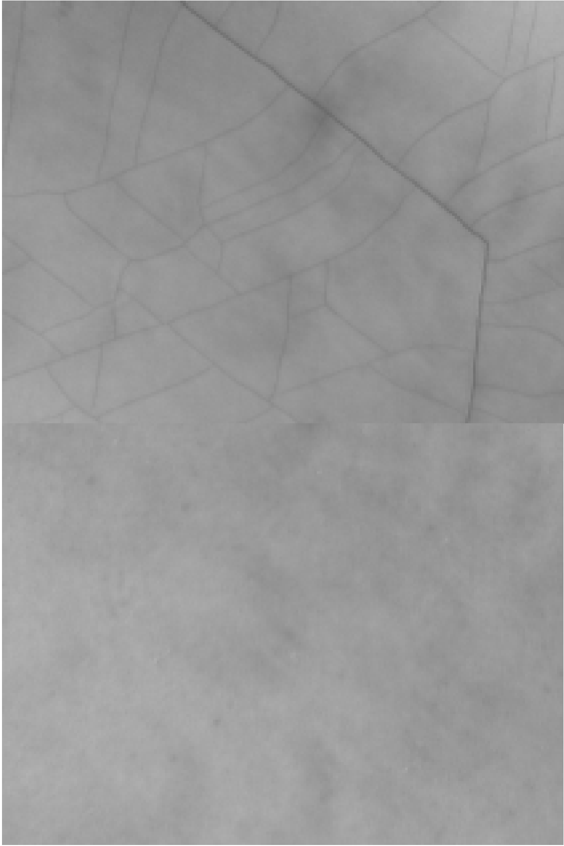

Fig. 16. AlN films grown by HVPE-technique according to traditional technology: (a) on Si; (b) on principle, new defect-free (at the expense of pores) SiC-bases on Si.

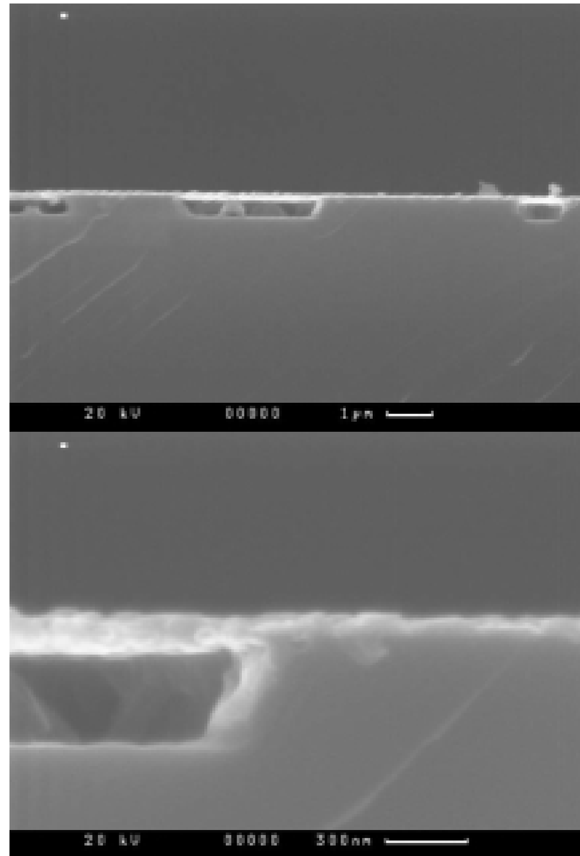

Fig. 17. Images of a section of SiC/Si-base of new type obtained by a raster electron microscope.

approximately 0.2 mm. Then, vapor of Si, being in equilibrium with solid Si both in the substrate and porous C, reacts chemically with carbon. According to Eq. (12) this resulted in formation of gaseous Si_2C, which flows to the Si-substrate, where it becomes absorbed. In the course of decomposition of mobile Si_2C-gas absorbed, formation of gaseous SiC takes place, and, along with, a process of nucleation and growth of solid SiC begins. Due to this process, in accordance with a general theory of nucleation, super saturation decreases and it becomes non-equilibrium. Then, SiC-nuclei formed grow and they are merged into a solid film. At 1250 °C, the process proceeds about 5-10 min, whereas, at higher temperatures, the process of solid layer formation is retarded, and, at lower temperatures, it proceeds more fast. Since then, evaporation of Si from the substrate is ceased, and the growth is carried out only due to silicon accumulated in porous Si. After some time, the reaction is terminated and the growth process of SiC film is completed. X-ray structural and electronographic investigations show that SiC-layers prepared on Si(111) by the above method are epitaxial and homogeneous over the whole substrate surface. Analysis of dependence of SiC-film thickness on the temperature of epitaxy at the 1100-1400 °C range shows that this relationship is well-described by Arrhenius curve of activation energy ~ 2.5 eV (note, that the film thickness is about 50 nm at T=1250 °C) and the above value of energy is approximated to the activation energy of desorption from the Si-surface, i.e. 2.6 eV. So, this fact proves the mechanism of epitaxy described above. Maximum concentration of SiC-islands in dependence with temperature is, also, described Arrhenius curve of activation energy ~ 1.5 eV.

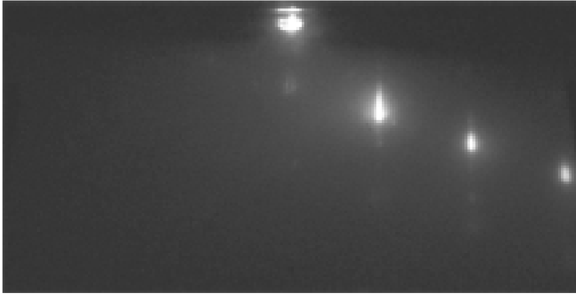

Fig. 18. Electronogram on reflection of high-energy electrons (75 kV) obtained for a base of new type. The type of electronogram conforms to practically perfect crystal structure of buffer AlN layer.

5.2. Experimental investigation of SiC- layers on Si

In order to provide effective wetting, a thin AlN-layer (~50-100 nm) is deposited on a substrate by HVPE technique. Substrates prepared in such a way are perfect bases for growth of GaN. GaN films grown on the substrates are of higher quality as compared to films on SiC. It should be underlined that a porous layer provides perfect correlation under thermal cooling, so that GaN films grown by the above-mentioned techniques do not undergo cracking. Patterns of GaN films grown by a traditional technique, i.e. on Si with a buffer layer of SiC and AlN, and on bases prepared by the new method described are given in Fig. 16.

In addition, our investigations show, that the films do not involve dislocations of mismatch of lattices at all, and they incorporate only twins of growth. Images of a section of SiC/Si –substrate obtained by a raster electron microscope is given in Fig. 17. The SiC-film of ~100 nm and pores in between it and silicon are well shown in the pattern. Just the pores provide relaxation of elastic strains. Electron reflection recording of the base is shown in Fig. 18.

Kikuchi-lines evidenced on perfect quality of the buffer layer can be distinguished by means of electronograph (note, that in figures made by a digital camera, the spectral lines are not seen).

27th of June of 2006 S.A. Kukushkin and A.V. Osipov presented a report on a new method of preparation of hexagonal single-crystal SiC polytype on Si-substrates of large diameter. The report [Resolution 62] was red on Bureau of meeting of Energetics, Mechanical Engineering, Mechanics and Controlling Processes Section of the Russian Academy of Sciences, Refs. [117,118]. The mentioned technique partly uses technical decisions developed in Refs. [109-112]. However, it is cardinally distinguished in the physics of Si-growth from all known technologies of film growing. The SiC films of cubic, hexagonal, and rhombohedral types can be grown by means of the technique developed and described in Refs. [117,118]. This is the first from published results in preparation of SiC of hexagonal polytypes on Si-substrates. The luminescence spectrum of hexagonal SiC coated on the porous Si-layer is given Fig. 19, Refs. [117,118]. It is shown that only 4H-polytype, i.e. hexagonal SiC, is present there and, therefore, wurtzite GaN and AlN-layers are readily laid on it.

Further, AlN/SiC-layers on Si (see Fig.16b) were coated with a thick GaN-layer by HVPE-technique at the growth rate of 2 μm/hour. The half-width of spectral rocking curve of the GaN-layer was equal to 10 arcmin. Now, we consider the structure and some properties (characteristics) of GaN-films grown by the new techniques described in Refs. [109-118].

6. GaN/SiC/Si STRUCTURES. SUPPRESSION OF CRACK-FORMATION PROCESS

So, at first a thin SiC-layer (~100 nm in thickness) was formed on Si(111) substrate by means of techniques described in Refs. [109-118]. Then, AlN (~300 nm in thickness) and, further, GaN (10-20 μm in thickness) layer chemically purified were grown by the technique similar to that described in Ref. [120].

The process of epitaxial GaN-layer formation, the quality of semiconductor structures prepared, and intermediate SiC/Si(111), AlN/SiC/Si(111) and GaN/AlN/SiC/Si(111)-structures included were estimated by means of optical and scanning electron microscopy methods (SEM-technique) Fig.18.

The presence of an interface disordered layer (about 3 μm in thickness) in a Si-substrate at SiC/Si -heteroboundary is shown in the image of GaN/AlN/SiC/Si(111) structure made by SEM-technique (Fig. 18). Appearance of the deformed layer is connected with pecularities of the processes of SiC formation on Si by the nonequilibrium heteroepitaxy technique described in [109-118], where Si-atoms react with C-atoms forming a layer (100 nm in thickness) with pores and microdefects included in silicon. It is well known long ago, that pores provide

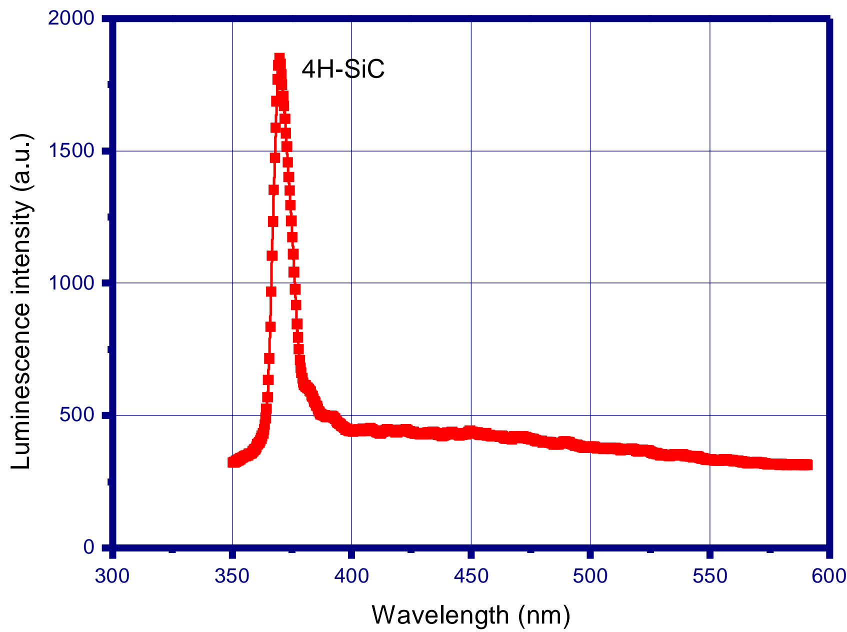

Fig.19. Luminescence spectrum of SiC coating on Si with a porous layer. It is shown that only 4H-polytype is present in this case. Just for the reason, wurtzite AlN and GaN-layers actively grow on it.

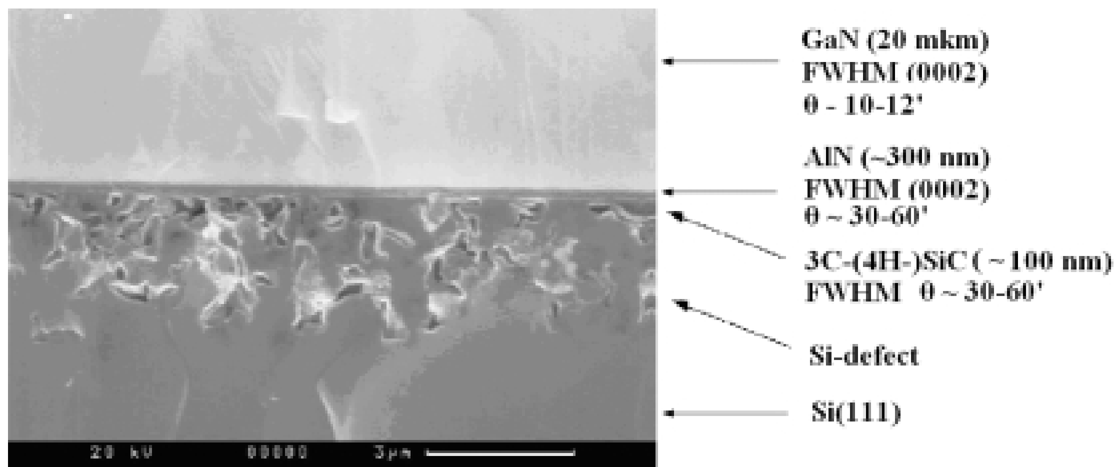

Fig. 20. SEM –image of GaN/AlN/SiC/Si structure fragment.

removal of elastic deformation in films [121-123]. However, both the mechanism of pore formation and that of relaxation of strains proposed by the authors of Refs. [109-118] are, in principle, differed from all the known techniques. The difference is associated with the fact that pores are not specially introduced into a substrate before growing a film on them. The pores are formed during SiC-growth, whereas their sizes and density cause to coincide them with the value of elastic energy in such a way that the film-substrate system ought to have an elastic energy minimum. Due to epitaxial growth of AlN-and GaN-layers by HVPE-technique for 2 hours at 1050 °C, the thickness of a disordered layer was increased from 100 nm up to a few microns (Fig. 20) and this fact promoted decreasing of deformation at SiC/Si heteroboundary.

X-ray diffraction measurements in successively grown layers of different thicknesses showed a decrease in disorientation in the GaN-layer as compared to an intermediate SiC-layer. The measured values of FWHM were as follows:

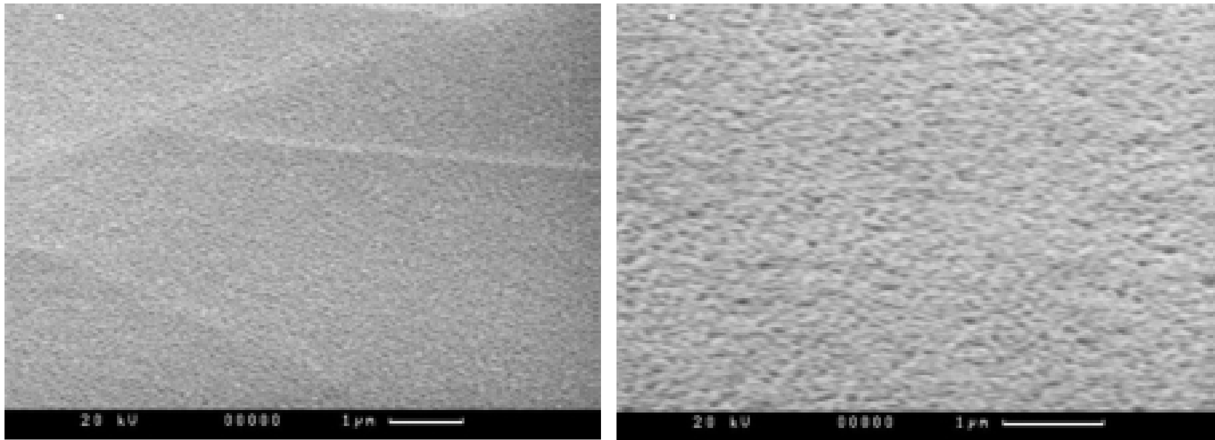

Fig. 21. SEM-images of surfaces for two structures AlN/Si (a) and AlN/SiC/Si (b) .

Table 8. Values of energy peak of the short-wave band of photoluminescence spectrum for GaN at room temperature, $h\nu_{300\hat{E}}$, and those of elastic strains in GaN-layers, σ_{xx} for some another structures prepared by HVPE method.

Structure	$h\nu_{300K}$ (eV)	Presence of cracks	σ_{xx}(GPa)	References
GaN/AlN/Si(111)	3.34	no	- 4.2	[68], [70]
GaN/AlN/SiC/Si(111)	3.38	no	- 2.9	[70]
GaN/6H-SiC	3.397	no	- 1,5	[71]
GaN/AlN/Si(111)	3.39	yes	- 1,8	[70]

- SiC (h~100 nm), ω_θ = 30-60 arcmin.

- AlN (h~300 nm), ω_θ = 30-60 arcmin.

- GaN (h~20 µm), ω_θ = 10-13 arcmin.

It should be noted that the half-width of X-ray diffraction rocking curves (FWHM) for SiC-films is sufficiently overestimated, since X-ray radiation penetrates not only into a film, because it is rather thin, but also the radiation affects the region (area, domain) of pores coated with disordered SiC-phase. In order to examine the structure of such layers, the authors of Refs. [109-118] used the electronographic technique based on diffraction of electrons from surfacial SiC-layers. By means of the above method, the quality of SiC/SiC(in pores)/Si-structure is conformed to high degree of certainty, and it shows high perfection of surfacial layers of SiC/Si-system.

Investigation of surfaces of AlN/SiC/Si-structures by means of optical and scanning electron microscope (SEM) shows that, in the case with AlN layers of about 300 nm in thickness, cracks are formed at a distance of a few nm from each other in a AlN/Si-structure, whereas in a AlN/SiC/Si-structure grown in the same way and of the same thickness of AlN-layer, the presence of similar cracks is not observed (Figs. 16b and 21b). As evidenced the result of investigation, in structures with application of SiC-layer, deformation of the structure is evidently decreased due to its relaxation at the stage of SiC-layer formation (Fig. 21).

The value of elastic deformation of GaN-layer was evaluated by disposition of energy maximum relative to short-wave band peak of photoluminescence, $h\nu_{300K}$, for three structures investigated at 300K. The following structures were analyzed In the experiments:

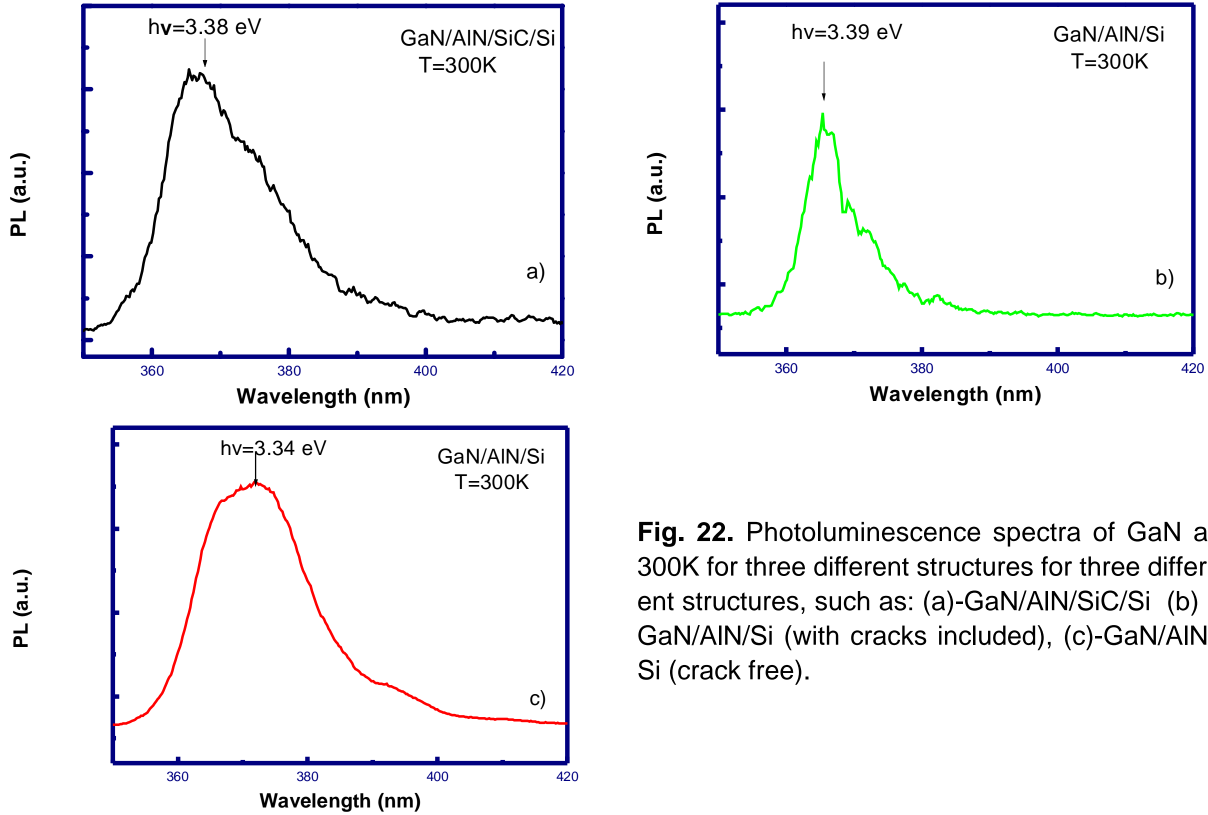

Fig. 22. Photoluminescence spectra of GaN at 300K for three different structures for three different structures, such as: (a)-GaN/AlN/SiC/Si (b) - GaN/AlN/Si (with cracks included), (c)-GaN/AlN/Si (crack free).

- GaN/AlN/SiC/Si (h_{GaN} ~ 10 µm), crack free, $h\nu_{300K}$ = 3.38 eV (Fig. 22 a),

- GaN/AlN/Si (h_{GaN} ~ 10 µm), with cracks included, $h\nu_{300K}$ = 3.39 eV (Fig.22 b)

- GaN/AlN/Si (h_{GaN} ~ 1 µm), crack free, $h\nu_{300K}$ = 3.34 eV (Fig. 22 c).

It can be shown that the energy of maximum of the photoluminescence spectrum is shifted to a short-wave band for GaN/AlN/Si-structures with cracks ($h\nu_{max}$ = 3.39 eV) as compared to structures without cracks ($h\nu_{max}$ = 3.34 eV). As for energy of maximum of the photoluminescence spectrum for GaN/AlN/SiC/Si structure ($h\nu_{max}$ = 3.39 eV), it is shifted to a short-wave band as well; however, lack of cracks apparently pointed to decrease in elastic deformation at the stage of formation of SiC layer. It is to be mentioned that energy of maximum of the photoluminescence for elastically-deformed GaN/AlN/Si structures is in agreement with the results described in Ref. [124].

As it is knows from Ref. [125], the energy of maximum of photoluminescence spectrum for GaN at room temperature is associated with elastic strains in the plane parallel to σ_{xx} heteroboundary, and it is described by the following relation:

$$h\nu_{300K}(eV)=3.4285+0.0211\sigma_{xx}(GPa) \quad (17)$$

Data on estimation of the elastic strain value in GaN-layers by means of Eq. (17) for GaN/AlN/SiC/Si(III) structures and structures prepared by HVPE technique, which are described in papers of another authors, are given in Table 8.

Estimations of σ_{xx} show that the layers are in the extension deformation state; however, the structure containing an intermediate layer has a lower value of elastic deformation. This points to the fact that elastic deformation of GaN/AlN/SiC/Si structure does not occur due to generation of cracks in an epitaxial layer, but it appears due to deformation relaxation at SiC/Si-boundary.

Note that our estimate of the elastic deformation value is of comparative character, because it

is rather higher than that of for similar structures, such as GaN/AlN/Si, obtained by Raman's spectroscopy in paper [96]. This fact is probably connected with an indirect character of evaluation of the value in accordance with photoluminescence data.

In addition, the pattern of luminescence used for the estimation of deformation value in a GaN layer and the pattern of luminescence spectrum of GaN layers allow to conclude that the film prepared in this case is of high quality. In photoluminescence spectra of the GaN layers at 77K, well-resolved bands are observed, namely, a narrow band (FWHM ~ 63 meV) of energy $h\nu_{max}$ = 3.45 eV and the "yellow" luminescence band associated with defects in the layer, $h\nu_{max}$ = 2.19 eV. A band with feature similar to those of previously reported in [126] for a base band was interpreted as the recombination band of an exciton bound to an acceptor. A low width of the exciton band and more high intensity of it as compared to that of the band associated with defects unambiguously point to a rather high quality of the GaN layer.

7. CONCLUSION

Thus, it should be concluded that a new approach for suppression the crack formation process along with decrease in elastic deformation for a GaN layer is promising in preparation of high quality GaN layer on a Si substrate. The approach is based on preparation of a thin SiC layer of hexagonal polytype on Si, where AlN and GaN layer are subsequently deposited on its surface [109-113].

8. ACKNOWLEDGMENTS

This work was supported by Russian Foundation for Basic Research (Grants: 06-03-32467 and 07-08-00542), St-Petersburg Scientific Center, RAS Projects (NFM—1/03, SS-2288.2003.1), RAS and Science and education Center "Quantum devices and nanotechnology" MIET, Federal contract 02.513.11.3152. The authors express deep gratitude to T.V. Lavrova for her help in designing of the paper, as well as, to E.A. Orlova for her help in translation of the paper from Russian into English.

REFERENCES

[1] S.D. Lester, F.A. Ponce, M.G. Craford and D.A. Steigerwald // *Appl. Phys. Lett.* **66** (1995) 1249.

[2] F.A. Ponce, In: *Group III Nitride Semiconductor Compounds*, ed. by B. Gil (Oxford University Press, Oxford, 1998) p. 123.

[3] E.V. Etzkorn and D.R. Clarke // *J. Appl. Phys.* **89** (2001) 1025.

[4] S.J. Pearton, F. Ren, A.P. Zhang and K.P. Lee // *Mater. Sci. Eng. Rep.* **R30** (2000) 55.

[5] T. Miyajima, T. Tojyo and T. Asano // *J. Phys. Cond. Matter* **13** (2001) 7099.

[6] R. Dimitrov, M. Murphy and J. Smart // *J. Appl. Phys.* **87** (2000) 3375.

[7] A. Fissel // *Phys. Rep.* **379** (2003) 149.

[8] M. Leszczynski, T. Suski and H. Teisseyre // *J. Appl. Phys*. **76** (1994) 4909.

[9] H. Amano, M. Iwaya and T. Kashima // *Jpn. J. Appl. Phys*. **37** (1998) L1540.

[10] B. Beaumont, Ph. Vennegures and P. Gibart // *Phys. Stat. Sol. (b)* **27** (2001) 1.

[11] T.S. Zheleva, S.A. Smith and D.B. Thomson // *J. Electron. Mater.* **28** (1999) L5.

[12] H. Lahreche, P. Vennegues, B. Beaumont and P. Gibart //*J. Cryst. Growth* **205** (1999) 245.

[13] C.I.H. Ashby, C.C. Mitchell and J. Han // *Appl. Phys. Lett.* **77** (2000) 3233.

[14] T. Detchprohm, M. Yano and S. Sano // *J. Appl. Phys.* **76** (1994) 4909.

[15] L.Liu and J.H.Edgar // *Mater.Sci.Eng.R* **37** (2002) 61.

[16] V.K.Nevolin, *Probe nanotechnologes in electronics* (Moscow, Technosfera, 2006), in Russian.

[17] M.P.Shaskolskaya, *Crystallography* (Moscow, Vuischaya Shkola,1984), in Russian.

[18] R.Z.Bakhtizin // *Light Emitting Diodes* **1** (2002) 77, in Russian.

[19] R.Z.Bakhtizin *Light Emitting Diodes* **1** (2002) 76, in Russian.

[20] H. Okumura, K. Ohta and G. Feuillet // *J. Cryst. Growth* **178** (1997) 113.

[21] E. Calleja, M.A. Sanchez-Garcia and F.J. Sanchez // *J. Cryst. Growth* **201/202** (1999) 296.

[22] D.M. Follstaedt, J. Han, P. Provencio and J.G. Fleming // *MRS Internet J. Nitride Semicond. Res.* **4S1** (1999) G3.72.

[23] Y.T. Rebane, Y.G. Shreter and W.N. Wang // *Appl. Surf. Solidi (a)* **166** (2000) 300.

[24] V.I. Trofimov, B.K. Medvedev, V.G. Mokerov and A.G. Shumynkov // *Proceeding of the Russian Academy of Sciences* **347** (1996) 469.

[25] V.I. Trofimov, B.K. Medvedev, V.G. Mokerov and A.G. Shumynkov // *Materials Research Society, Symposium Proceeding* **399** (Boston, USA, 1995) p. 47.

[26] B.K. Medvedev, V.G. Mokerov and N.V.Peskov // *Technical Physics Letter* **20** (1994) 20.

[27] A.Koukitu , J. Kikuchi, Y.Kangawa and Y.Kumagai // *J. Crystal Growth* **281** (2005) 47.

[28] V.N.Bessolov, Yu.V. Zhilyaev and H.S.Park, *Method of manufacture of epitaxial GaN layer on Si* , Applied patent N2006127075 date 25.07.2006.

[29] H.P. Maruska and J.J.Tietjen // *Appl. Phys. Lett.* **15** (1969) 327.

[30] R. Dingle, K.L.Shakla, R.F.Leheny and R.B.Zetterstrom // *Appl. Phys. Lett.* **19** (1971) 5.

[31] J.I. Pankove and J. Lumin // *Appl. Phys. Lett.* **4** (1971) 63.

[32] Y. Ohki // *Inst. Phys. Conf. Ser.* **63** (1981) 479.

[33].H. Amano, N.Sawaki, I.Akasaki and Y.Toyoda // *Appl. Phys. Lett.* **48** (1986) 353.

[34] H. Amano // *J. Appl. Phys.* **29** (1990) L205.

[35] H. Amano // *J. Electrochem. Soc.* **137** (1990) 1639.

[36] H. Amano // *Mater. Res. Soc. Ext. Abstr.* **EA-21** (1990) 165.

[37] H. Murakami //*J. Crystal Growth* **115** (1991) 648.

[38] S. Nakamura // *Jpn. J. Appl. Phys.* **36** (1997) L1568.

[39] S. Nagahama // *Jpn. J. Appl. Phys.* **39** (2000) L647.

[40] S.Nakamura and G.Fasol, *The blue laser diodes* (Berlin: Springer, 1998).

[41] Y.Morkoc, *Wide band gap nitrides and devices* (Berlin: Springer, 1998).

[42] Yu.G.Sreter, Yu.T.Rebane, V.A.Zukov and V.G.Sidorov, *Wide band gap semiconductors* (S-Petersburg, 2001).

[43] I.Akasaki // *J.Cryst.Growth* **300** (2007) 2.

[44] S.-N.Lee, S.Y.Cho, H.Y.Ryu, J.K.Son, H.S.Paek, T.Sakong, T.Jang, K.K.Choi, K.H.Ha, M.H.Yang, O.H.Nam and Y.Park // *Appl. Phys Lett.* **88** (2006) 111101.

[45] C.-F.Lin, J.H.Zheng, Z.-J.Yang, J.-J.Dai, D,-Y.Lin, C.-Y.Chang, Z.X.Lai and C.S.Hong // *Appl. Phys. Lett*. **88** (2006) 083121.

[46] K.H.Kim, K.S.Jang, S.L.Hwang, H.S.Jeon, W.J.Choi, M.Yang, H.S.Ahn, S.W.Kim, Y.Honda, M.Yamaguchi, N.Sawaki, J.Yoo, S.M.Lee and M.Koike // *Phys.Stat.Solidi.* **4** (2007) 29.

[47] Z.Ren, Q.Sun, S.-Y.Kwon, J.Han, K.Davitt, Y.K.Song, A.V.Nurmikko, W.Liu, J.Smart and L.Schowalter // *Phys.Stat.Solidi.* **4** (2007) 2482.

[48] T.Palacios , L.Shen, S.Keller, A.Chakraborty, S.Heikman, S.P.DenBaars and U.K.Mishra // *Appl.Phys.Lett.* **89** (2006) 073508.

[49] Y.Taniyasu, M.Kasu and T.Makimoto // *Nature* **441** (2006) 325.

[50] G.H.Jessen, J.K.Gillespie, G.D.Via, A.Crespo, D.Langley, M.E.Aumer, C.S.Ward, H.G.Henry, D.B.Thomson and D.P.Partlow // *IEEE Electron. Dev. Lett.* **28** (2007) 354.

[51] J.H.Kim and P.H.Holloway // *Adv. Mater.* **17** (2005) 91.

[52] F. Bernardini ,V.Fiorentini and D.Vanderbilt // *Phys.Rev. B* **56** (1997) R10024.

[53] P.Waltereit, O.Brandt, A.Trampert, H.T.Grahn, J.Menniger, M.Ramsteiner, M.Reiche and K.H.Ploog // *Nature* **406** (2000) 865.

[54] Y. J. Sun, O. Brandt, S. Cronenberg, S. Dhar, H. T. Grahn, K. H. Ploog, P. Waltereit and J. S. Speck // *Phys.Rev.B* **67** (2003) 041306.

[55] N.M. Ng // *Appl.Phys.Lett.* **80** (2002) 4369.

[56] A. Chitnis, C. Chen, V. Adivarahan, M. Shatalov, E. Kuokstis, V. Mandavilli, J. Yang and M. Asif Khan // *Appl.Phys.Lett.* **84** (2004) 3663.

[57] P.R.Taverni, B.Imer, S.P.DenBaars and D.R.Clarke // *Appl.Phys.Lett.* **85** (2004) 4630.

[58] *Growth of planar non-polar {1-100} m-plane GaN with MOCVD*, US Patent 20060270087, May 31 2006.

[59] *Defect reduction of non-polar and semi-polar III-nitrides with sidwall lateral epitaxial overgrowth (SLEO)*, US Patent 20060270076, May 31 2006.

[60] A. Benjamin // *J.of Electron.Mater.* **34** (2005) 367.

[61] B.A.Haskell // *APL* **86** (2005) 111917.

[62] D.F.Feezell, M.C.Schmidt, R.M.Farrell, K.-C.Kim, M.Sakato, K. Fujito, D.A.Cohen, J.S.Speck, S.P.DenBaars and S.Nakamura // *Jap.Journ. Appl. Phys.* **46** (2007) L284.

[64] M.C.Schmidt, K.-C.Kim, R.M.Farrell, D.F.Feezell, D.A. Cohen, M.Saito, K.Fujito,

J.S.Speck, S.P.DenBaars and S.Nakamura // *Jap.Journ. Appl. Phys.* **46** (2007) L190.

[65] K. Iso, H. Yamada, H.Hirasawa, N. Fellows, M. Saito, K., S. P. DenBaars, J. S. Speck and S. Nakamura // *Jap.Journ. Appl. Phys.* **46** (2007) L960.

[66] J.H.Song, Y.Z.Yoo, K.Nakajima, T.Chikyow, T.Sekiguchi and H.Koinuma // *J.Appl.Phys.* **97** (2005) 043531.

[67] A.Nashimoto, Y.Asiba, T.Motizuki, M.Ohkubo and A.Yamamoto // *J.Cryst.Growth* **175/176** (1997) 129.

[68] F.Yun, Y.-T. Moon, Y.Fu.K.Zhu, U.Ozgur and H.Morkoc // *J.Appl.Phys.* **98** (2005) 123502.

[69] A.Dadgar// *IPAP conference Series 1* (2000) 845.

[70] P. Chen // *J.Cryst.Growth.* **225** (2001) 150.

[71] K.H.Lee, M.H.Hong, K.Teker, C.Jacob and P.Pirouz // *Mater.Res.Soc.Symp.Proc. (Pittsburgh: MRS)* **622** (2000) p. 72.

[72] X.Xu, R.Armitage, S.Shinkai, K.Sasaki, C.Kisielowski and E.R.Weber // *Appl.Phys.Lett.* **86** (2005) 182104.

[73] J.Tolle, J.Konvetakis, D.-W. Kim, S. Mahajan, A.Bell, F.A.Ponce, I.S.T. Tsong, M.L.Kottke and Z.D.Chen // *Appl.Phys.Lett.* **84** (2004) 3510.

[74] H.W.Kim and N.H.Kim // *Appl. Surf. Sci.* **236** (2004) 192.

[75] Y.Wu, X.Han, J.Li, D.Li, Y.Lu, H.Wei, G.Cong, X.Liu, Q.Zhu and Z.Wan // *J. Crystal Growth.* **279** (2005) 335.

[76] W.-Y. Uen, Z.,-Y .Li, S.-M. Lan and S.-M. Liao // *J. Crystal Growth* **280** (2005) 335.

[77] N.H.Zhang, X.L.Wang, Y.P.Zeng, H.L.Xiao, J.X.Wang, H.X.Liu and J.M.Li // *J. Crystal Growth* **280** (2005) 346.

[78] A.J.Steckl, J.Devrajan, C. Tran and R.A.Stall // *Appl.Phys.Lett.* **69** (1996) 2264.

[79] J.Komiyama, Y. Abe, S. Suzuki and H. Nakanishi // *Appl.Phys.Lett.* **88** (2006) 091901.

[80] A.Dadgar // *Appl.Phys.Lett.* **78** (2001) 2211.

[81] A.Krost and A.Dadgar // *Phys.Status.Solidi (a).* **194** (2002) 361.

[82] S.Radhavan and J.M.Redwing // *J. Appl.Phys.* **98** (2005) 023514.

[83] W.G.Perry // *Mater.Res.Soc.Symp.Propc.* **415** (1997) 3.

[84] J.E.Nortrup and J.Neugebauer // *Phys.Rev.B* **53** (1996) R10477.

[85] M.D.Drory, J.W.Ager III, T.Suski, I.Grzegory and S.Porowski // *Appl.Phys.Lett.* **69** (1996) 4044.

[86] P.R.Tavernier, P.M.Verghese and D.R.Clarke // *Appl.Phys.Lett.* **74** (1999) 2678.

[87] E.V.Etzkorn and D.R.Clarke // *J.Appl.Phys.* **89** (2001) 1025.

[88] E.Feltin, B.Beaumont, P.Vennegues, T.Riemann, J.Christen, J.P.Faurite and P.Gibart // *Phys. Stat. solidi (a).* **188** (2001) 531.

[89] S.Zamir, B.Meyler and J.Salzman // *Appl.Phys.Lett.* **78** (2001) 288.

[90] K.-J. Kim and C.-R. Lee // *J.Korean Physical Soc.* **46** (2005) 901.

[91] N.H.Zhang, X.L.Wang, Y.P.Zeng, H.L.Xiao, J.X.Wang, H.X.Liu and J.M.Li // *J.Phys.D: Appl.Phys.* **38** (2005) 1888.

[92] D.Wang, M.Ichikawa and S.Yoshida // *Appl.Phys.Lett.* **80** (2002) 2472.

[93] D.Wang, Y.Hiroyama, M.Tamura, M.Ichikawa and S.Yoshida // *Appl.Phys.Lett.* **77** (2000) 1846.

[94] A.Dadgar, C.Hums, A.Diez, J.Blasing and A.Krost // *J.Cryst. Growth.* **297** (2006) 279.

[95] K.L.Lin // *Tech. program.Intern.Cohfer.Nitrid. Semic., September 2007, USA*, TP85.

[96] V.N.Bessolov, V.Yu.Davydov, Yu.V.Zhilyaev, E.V.Konenkova, G.N.Mosina, S.D.Raevskii, S.N.Rodin, Sh.Sharofidinov, M.P.Shcheglov, Hee Seok Park and M.Koike // *Technical Physics Letter* **31** (2005) 915.

[97] J.X.Zhang, Y.Qu, Y.Z.Chen, A.Uddin and S.Yuan // *J.Cryst. Growth* **82** (2005) 137.

[98] K.J.Lee, E.H.Shin, S.K.Shim, T.K.Kim, G.M.Yang and K.Y.Lim // *Phys.stat.sol. C* **2** (2005) 2104.

[99] E.Tuomisto, T.Paskova, R.Kroger, S.Figge, D.Hommel, B.Monemar and R.Kersting // *Appl.Phys.Lett.* **90** (2007) 121915.

[100] A.Vescan, J.D. Brown J.W. Johnson, R. Therrien, T. Gehrke, P. Rajagopal, J.C. Roberts, S. Singhal, W. Nagy and R. Borges // *Phys. Stat. Sol.(c)* **20** (2002) 52.

[101]. S.Arulkumaran, T.Egawa, S.Matsui and H.Ishikawa // *Appl.Phys.Lett.* **86** (2005) 123503.

[102] F.Semond, P.Lorenzini, N.Grandjean and J.Massies // *Appl.Phys.Lett.* **78** (2001) 335.

[103] J.Schalwiga, G.Muller, U.Karrer, M.Eickhoff, O.Ambacher, M.Stutzmann,

L.Gorgens and G.Dollinger // *Appl.Phys.Lett.* **80** (2002) 1222.

[104] J.S.Thakur, H.E.Prakesam, L.Zhang, E.F.McCullen, L.Rinai, V.M.Garcia-Snarez, R.Naik, K.Y.S.Ng and G.W.Auner // *Phys.Rev.B* **75** (2007) 075308.

[105]. S.Guna and N.A.Bojarczuk // *Appl.Phys.Lett.* **72** (1998) 415.

[106] C.A.Tran, A.Osinski, R.F.Karlichek and I.Berishev // *Appl.Phys.Lett.* **75** (1999) 1494.

[107] F.Schulze, A.Dadgar, F.Berttram, J.Blasing, A.Diez, P.Veit, R.Cios, J.Christen and A.Krost // *Phys.Stat.Solidi.* **4** (2007) 41.

[108] Z.Ye, X.Gu J.Huang, Y.Wang, Q.Shao and B.Zhao // *Intern.J.Modern.Physics B* **16** (2002) 4310.

[109] S-J.Park, H-B.Lee, W.L.Shan, S-J.Chua, J.-H. Lee and S-H.Hahm // *Phys.stat.solidi.* **2** (2005) 2559.

[110] X.Wang, X.Wang, B.Wang, H.Xiao, H.Liu, J.Wang, Y.Zeng and J.Li // *Phys.stat.solidi.* **4** (2007) 1613.

[111] Y. Khlebnikov, I. Khlebnikov, M. Parker and T.S. Sudarshan // *J. Cryst. Growth.* **233** (2001) 112.

[112] A.R. Bushroa, C. Jacoba, H. Saijoa and S. Nishino // *J. Cryst. Growth* **271** (2004) 200.

[113] S. A. Kukushkin, A. V. Osipov, V. P. Rubets, S. K. Gordeev and S. B. Korchagina // *Technical Physics Letters* **31** (2005). 859.

[114] A. P. Belyaev, S. A. Kukushkin, A. V. Osipov, V. P. Rubets, S. K. Gordeev and S. B. Korchagina // *Technical Physics Letters* **32** (2006) 414.

[115] S. K. Gordeev, S. B. Korchagina, S. A. Kukushkin and A. V. Osipov, *RF Patent Appl.* No. 2286616 (October 2006, 27).

[116] S. K. Gordeev, S. B. Korchagina, S. A. Kukushkin and A. V. Osipov, *RF Patent Appl.* No. 2286617 (October 2006, 27).

[117] S. A. Kukushkin and A. V. Osipov, *Nano silicon carbide on silicon: new material for opto- and micro-electronics. Bureau of meeting of Energetics, Mechanical Engineering, Mechanics and Controlling Processes Section of Russian Academy of Sciences* (Resolution N 62 from 27.06. 2006).

[118] S. A. Kukushkin and A. V. Osipov // *Physics of the Solid State* **50** (2008), in print.

[119] I. G. Aksyanov // *Technical Physics Letters* (2008), in print.

[120] V. N. Bessolov // *Technical Physics Letters* **32** (2006) 60.

[121] S.Nishino, J.A. Powell and H.A. Will // *Appl.Phys.Lett.* **42** (1983) 460.

[122] E. Bustarret, D. Vobornik, A. Roulot, T. Chassagne, G. Ferro, Y. Monteil, E. Martinez-Guerrero, H. Mariette, B. Daudin and Le Si Dang // *Phys.stat.sol. (a)* **195** (2003) 18.

[123] M. G. Mynbaeva // *Technical Physics Letters* **32** (2006) 25.

[124] J.X. Zhang, Y. Qu, Y.Z. Chen, A. Uddin and Shu Yuan // *J. Cryst. Growth.* **282** (2005) 137.

[125] A.Yamamoto, T. Yamauchi, T. Tanikawa, M. Sasase, B.K. Ghosh, A. Hashimoto and Y. Ito // *J. Cryst. Growth* **261** (2004) 266.

[126]. M. Kuball, J.M.Hayesw, A.D.Prins, N.W.A. van Uden, D.J.Dunstan, Y.Shi and J.H.Edgar // *Appl. Phys. Lett.* **78** (2001) 724.